PROBABILISTIC-GRAPHICAL AND PHENOMENOLOGICAL ANALYSIS OF COMBINED BENDING-TORSION FATIGUE RELIABILITY DATA

by

Dr. Dimitri Kececioglu and Hugh Broome

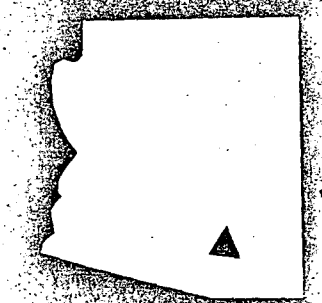

ENGINEERING EXPERIMENT STATION
COLLEGE OF ENGINEERING
THE UNIVERSITY OF ARIZONA
TUCSON, ARIZONA

91 p

72839

NASA CONTRACTOR
REPORT

NASA CR-~~XXX~~

NASA CR-XXX

PROBABILISTIC-GRAPHICAL AND PHENOMENOLOGICAL ANALYSIS OF COMBINED BENDING-TORSION FATIGUE RELIABILITY DATA

by Dr. Dimitri Kececioglu and Hugh W. Broome

Prepared under Grant No. NGL- 03-002-044 by The University of Arizona

Tucson, Arizona

for

NATIONAL AERONAUTICS AND SPACE ADMINISTRATION - WASHINGTON, D. C.

PROBABILISTIC-GRAPHICAL AND PHENOMENOLOGICAL ANALYSIS OF COMBINED BENDING-TORSION FATIGUE RELIABILITY DATA

by

Dr. Dimitri Kececioglu and Hugh W. Broome

Prepared For

NATIONAL AERONAUTICS AND SPACE ADMINISTRATION

July 30, 1969

Grant NGR 03-002-044

Project Management
NASA-Lewis Research Center
Cleveland, Ohio

Vincent R. Lalli

College of Engineering
THE UNIVERSITY OF ARIZONA
Engineering Experiment Station
Tucson, Arizona

ABSTRACT

Fatigue data generated by three combined bending-torsion fatigue reliability research machines at The University of Arizona are probabilistic-graphically and phenomenologically analyzed. Distributions that are applicable to fatigue life and static strength data are discussed. Phenomenological justifications for the use of these distributions are presented.

It is found that the normal distribution represents the cycles-to-failure data at the highest stress levels best. The lognormal distribution appears to fit the cycles-to-failure data at the lower stress levels best and quite well at all stress levels including the highest.

A regression analysis and least-squares goodness-of-fit test was performed for normal and lognormal plots. In most cases, the correlation coefficient gave a better fit to the data using the normal distribution, but the difference between the two was so slight that positive discrimination could not be made.

From the probabilistic-graphical analysis and the phenomenological reasoning, it was concluded that the lognormal distribution gave a very satisfactory fit to the cycles-to-failure data at all stress levels, that the normal distribution could be used to represent the cycles-to-failure at the highest stress levels without any loss of accuracy.

The normal distribution is found to describe the static strength distributions best.

The Weibull distribution was also studied and the probabilistic-graphical plots were found not to lend themselves to as good a straight line fit to the cycles-to-failure data as desired. The plots had many kinks that could not be straightened by adjusting the location parameter. Phenomenologically it was found that the Weibull

would be the best distribution if the cycles-to-failure data were those of only the failed items in a large sample or of field failures because these would be the failures of the weakest in a sample thus conforming to the extreme-value Weibull distribution theory.

TABLE OF CONTENTS

LIST OF ILLUSTRATIONS

LIST OF TABLES

SYMBOLS

Symbol	English
c	Cycles
c.d.f.	Cumulative distribution function
E(x)	Expected value of a random variable
F(x)	Cumulative distribution function
f(x)	Probability density function
g(x)	Fatigue life length p.d.f.
n	Sample size
p.d.f.	Probability density function
r_s	Stress ratio
s_a	Alternating stress
s_m	Mean stress
var	Variance
x	Random variable
∞	Infinity
$*$	Convolution operator

Symbol	Greek
α_3	Coefficient of skewness
α_4	Coefficient of kurtosis
β	Shape of parameter
$\Gamma(n)$	Gamma function evaluated at n
γ	Location parameter

Symbol	Greek
δ_i	Proportionality constant
η	Scale parameter
μ_1	Mean of a random variable
μ_2	Second moment about the mean or variance
μ_3	Third moment about the mean or skewness
μ_4	Fourth moment about the mean or kurtosis
μ_K	Kth moment of a distribution about the mean
μ_i	$E(x^i)$ for i = 2, 3, . . .
μ''	Mean of the logarithms of a random variable
σ	Standard deviation = $(Var)^{1/2}$
σ_a	Maximum alternating bending stress
σ''	Standard deviation of the logarithms of a random variable
τ_m	Maximum mean shear stress

I SUMMARY

Three combined-stress fatigue reliability research machines have been built and calibrated to test relatively large specimens under combined reversed-bending and steady-torque loading conditions. These machines are generating data to be used in determining statistical strength surfaces (three-dimensional Goodman diagrams) so that specified reliabilities may be designed into components subjected to such combined loading using the design by reliability methodology.

This report is based on the results from 170 test specimens which yielded cycles-to-failure, stress-to-failure, and endurance strength data at various stress levels and at the alternating stress to mean stress ratios of ∞, 0.70, 0.90, and 0. The specimens were made of SAE 4340 Steel of Rockwell 35 to 40 hardness on Scale C, and processed according to MIS-S-5000B, MIL-H-6875, and MIL-I-6868.

Specimens were tested at five levels of alternating stress for the stress ratio of ∞, i.e., 154,000 psi, 121,000 psi, 104,500 psi, 87,000 psi, and 78,000 psi. Eighteen specimens were tested at each of the four lower stress levels and twelve specimens at the highest level. Specimens were tested at four levels of alternating stress for the stress ratio of 0.70, i.e., 110,500 psi, 97,500 psi, 76,000 psi, and 70,000 psi. Eighteen specimens were tested at each of the three lower levels and twelve specimens at the highest level.

Ten notched and ten unnotched specimens were statically tested to failure for the stress ratio of 0, and the ultimate strength was determined.

The Weibull, normal and lognormal distributions were fitted to the cycles-to-failure and ultimate strength data. Graphical-

probabilistic and phenomenological analysis was made of the data to decide which statistical distribution best represents them.

The normal and lognormal distributions gage good fits to the cycles-to-failure data for the stress ratios of ∞ and 0.70. The Weibull distribution, although very versatile, is an extreme-value distribution and does not exactly reflect the results of this research. Phenomenological reasons favored the lognormal over the normal distribution to best represent the cycles-to-failure data at all stress levels. At the highest stress levels, however, the normal distribution can be used to approximate the lognormal distribution. This can be justified both probabilistic-graphically and phenomenologically.

The static ultimate strength data of the notched specimens (stress ratio of 0) were found to be best represented by the normal distribution both graphically and phenomenologically.

II INTRODUCTION

When a specimen is subjected to an alternating stress, even a stress below the static fracture strength, cracks will form and propagate to cause rupture or failure. This phenomenon is called fatigue, and the rupture is referred to as a fatigue failure. If the same level of alternating stress is applied to several specimens, the scatter in the number of cycles necessary to produce fatigue failure is quite large.

This scatter exceeds experimental error, and many testing programs have been executed which show the scatter cannot be explained by differing surface finishes, heat treatments, or inhomogeneity of the material. Physicists, metallurgists, and applied mathematicians have proposed various theories which place a significance on the scatter from a statistical viewpoint.

The fact that this scatter in cycles-to-failure at a constant stress level exists has been known for a long time. It has only been quite recently, however, that the statistical nature of fatigue has been recognized. It is now considered a fundamental and essential characteristic of fatigue analysis.

For three years, fatigue testing, under the combined effects of alternating bending and mean torque, has been carried on at The University of Arizona. This testing was done under the direction of Dr. Dimitri Kececioglu and the sponsorship of the National Aeronautics and Space Administration.

The testing has been carried out on combined bending-torsion, fatigue reliability research machines designed and built at The University of Arizona. These machines are capable of applying and maintaining an alternating bending stress and a mean shear stress at different levels in a rotating round specimen. The machines and

specimens are described in detail in previous reports (1, pp. 193-257), (2). The test specimens were notched with a theoretical stress concentration of 1.45 and were of SAE 4340 Steel.

The tests were conducted at various alternating bending stress levels while holding constant alternating-stress-to-mean stress ratios. The purpose was to determine statistically the effects of superposing steady torque onto bending on the S-N diagram for such constant stress ratios. Testing has been completed for three stress ratios: ∞, 0.70 (0.90 for endurance) and 0. The data and results are given in Tables 1, 2 and 3 and Figures 1 and 2.

The data can be used to generate statistical distributions of cycles-to-failure and a statistical S-N diagram at each stress ratio as shown in Figures 1 and 2. This information can also be used to determine the strength of the specimens at specific cycles of life as shown in Figure 3.

After data for several stress ratios have been gathered, a statistical Goodman surface for the fatigue strength of a specimen at specific cycles of life for various stress ratios can be generated as shown in Figure 4.

The stress ratio, r_s, is defined as

$$r_s = \frac{s_a}{s_m}. \tag{1}$$

For The University of Arizona research program the alternating stress is a bending stress, and the mean stress is a shear stress. Using the von Mises-Hencky theory of failure $s_a = \sigma_a$ and $s_m = \sqrt{3}\,\tau_m$ (2, p. 87), the stress ratio then becomes

$$r_s = \frac{\sigma_a}{\sqrt{3}\,\tau_m}. \tag{2}$$

A. Stress Ratio of ∞

To test a ratio of ∞ is to test the specimens with pure bending stress only and zero shear stress. This was done at five levels of alternating stress and the cycles-to-failure were determined. Testing was also done, using the staircase method (3, pp. 113-114), to find the endurance strength of the notched specimens. The results are presented and discussed in a previous report (2).

The alternating stress levels at $r_s = \infty$ were

$$s_{a_1} = 154{,}000^{*} \text{ psi},$$

$$s_{a_2} = 121{,}500 \text{ psi},$$

$$s_{a_3} = 104{,}500 \text{ psi},$$

$$s_{a_4} = 87{,}000 \text{ psi},$$

$$s_{a_5} = 78{,}000 \text{ psi}.$$

The cycles-to-failure at these various alternating stress levels are given in Table 1. The results are given in Figure 1.

---

*These stresses are rounded out to the nearest 500 psi.

B. Stress Ratio of 0.70

To test at a stress ratio of 0.70, various levels of alternating bending stress were used with the mean shear stress adjusted to maintain the constant ratio. Four levels of alternating stress were used. They were

$$s_{a_1} = 110{,}500 \text{ psi},$$

$$s_{a_2} = 97{,}500 \text{ psi},$$

$$s_{a_3} = 76{,}500 \text{ psi},$$

$$s_{a_4} = 70{,}000 \text{ psi}.$$

Using the von Mises-Hencky theory, the shear stress at each level was $\tau_1 = 88{,}500$ psi, $\tau_2 = 80{,}500$ psi, $\tau_3 = 65{,}000$ psi, $\tau_4 = 57{,}000$ psi, to maintain a stress ratio of 0.70. The cycles-to-failure data are given in Table 1. The staircase method was used to determine the distribution of the endurance strength at a stress ratio of 0.90. The results are given in Figure 2.

C. Stress Ratio of 0

To determine the distribution for stress ratio of 0, twenty specimens were tested to failure under tensile loading. Ten of the specimens were regular notched specimens and ten were unnotched with a diameter equal to the diameter at the base of the notch. The results are given in Tables 2 and 3.

The strength distribution for a stress ratio of 0 was taken to be the ultimate strength distribution for the notched specimens. The ultimate is the end of the load carrying ability of the specimen, and this is of interest to the design engineer. The ultimate strength, as the intersection of the modified Goodman line and the abscissa, agrees with the literature (2, pp. 20-23),(4, p. 180),(5, p. 178),(6,p. 270). Figure 4 reflects the use of this conclusion.

III. THE DENSITY FUNCTIONS, MOMENTS AND PARAMETERS OF STATISTICAL DISTRIBUTIONS

A. Density Functions

The cumulative distribution, $F(x_i)$, of a random variable x is the probability that x assumes a value no greater than some specified x_i, or

$$F(x_i) = \text{Probability } (x \leq x_i). \tag{3}$$

The probability density function f(x) is defined as

$$f(x) = \lim_{\Delta x_i \to 0} \frac{\text{Probability } (x_i \leq x \leq x_i + \Delta x_i)}{\Delta x_i}$$

or

$$f(x) = \frac{d}{dx}[F(x)]. \tag{4}$$

It follows from the definition of the probability density function that

$$\int_{-\infty}^{\infty} f(x)dx = F(x)\Big|_{-\infty}^{\infty} = F(\infty) - F(-\infty) = 1 - 0 = 1,$$

or the area under the probability density function is equal to one. Also it should be noted that the cumulative distribution can be obtained from the probability density function as follows:

$$F(t) = \int_{-\infty}^{t} f(x)dx. \qquad (5)$$

The probability density function is referred to as the pdf, and the cumulative distribution function as the cdf.

B. Expected Values and Moments of Distributions

The expected value of a distribution, or the mean of a random variable x, is of interest in analyzing distributions. This is given by

$$E(x) = \int_{-\infty}^{\infty} xf(x)dx = \mu_1. \tag{6}$$

The K^{th} moment of the distribution about the mean, μ_K, is given by

$$\mu_K = E(x-\mu_1)^K = \int_{-\infty}^{\infty} (x-\mu_1)^K f(x)dx. \tag{7}$$

These moments about the mean can sometimes be simplified if it is noted that

$$E(\Sigma x_i) = \Sigma[E(x_i)], \tag{8}$$

and

$$E(cx) = c \cdot E(x). \tag{9}$$

The second moment about the mean, a measure of the spread or dispersion of the distribution, is called the variance (μ_2) and is obtained as follows

$$\mu_2 = E(x-\mu_1)^2 \tag{10}$$

or

$$\mu_2 = E(x^2) - 2\mu_1 E(x) + (\mu_1)^2.$$

But

$$E(x) = \mu_1, \tag{11}$$

and

$$E(x^2) = \mu_2'. \tag{12}$$

Therefore,

$$\mu_2 = \mu_2' - (\mu_1)^2. \tag{10a}$$

The third moment about the mean, called the skewness (μ_3), is a measure of the symmetry of the distribution and is given by

$$\mu_3 = E(x-\mu_1)^3, \tag{13}$$

$$\mu_3 = \mu_3' - 3\mu_2'\mu_1 + 2\mu_1^3. \tag{13a}$$

The coefficient of skewness, α_3, is defined as

$$\alpha_3 = \mu_3/(\mu_2)^{3/2}, \tag{14}$$

and is a measure of the skewness relative to the spread of the distribution. If $\alpha_3 > 0$, the distribution is skewed to the right. This means that a tail extends to the left. If $\alpha_3 < 0$, the distribution is skewed to the left, and if $\alpha_3 = 0$, the distribution is symmetrical.

The fourth moment about the mean, called the kurtosis (μ_4), is a measure of the peakedness of the distribution, and is given by

$$\mu_4 = E(x-\mu_1)^4, \tag{15}$$

$$\mu_4 = \mu_4' - 4\mu_3'\mu_1 + 6\mu_2'(\mu_1)^2 - 3(\mu_1)^4. \tag{15a}$$

The coefficient of kurtosis is defined as

$$\alpha_4 = (\mu_4)/(\mu_2)^2. \tag{16}$$

The value of α_4 is used to measure the peakedness of distributions relative to each other. The distribution with the largest α_4 is the most peaked.

IV. DISTRIBUTIONS APPLICABLE TO FATIGUE

The statistical distributions which are frequently used in, and those which have been successfully applied to, the explanation of fatigue phenomena are the following:

1. Gaussian or normal
2. Lognormal
3. Gamma
4. Erlangian
5. Exponential
6. Extreme-value
7. Weibull
8. Beta

The choice of the appropriate distribution to be applied to specific fatigue phenomena has to be based on the statistical, as well as, the phenomenological aspects of the generated fatigue data. These aspects are discussed next.

A. The Normal Distribution

The normal is the most widely used of all distributions. It is best described as the distribution of events which are the result of the sum of many small effects. Many random events are not normally distributed, and therefore there would be no reason to expect a normal distribution. However, one justification for examining the normal is the central limit theorem.

The central limit theorem states that the distribution of the mean of n independent observations from any distribution with finite mean and variance approaches a normal distribution as the number of observations, n, approaches ∞. This is an important principle, because although it applies to a large number of observations, even a relatively small number of observations will tend to normality if the parent distribution does not deviate too far from the normal.

The probability density function of the normal distribution is given by

$$f(x: \mu, \sigma) = \frac{1}{\sigma\sqrt{2\pi}} \exp\left[-\tfrac{1}{2}\left(\frac{x-\mu}{\sigma}\right)^2\right]. \qquad (17)$$

The mean is given by

$$E(x) = \frac{1}{\sigma\sqrt{2\pi}} \int_{-\infty}^{\infty} x \exp\left[-\tfrac{1}{2}\left(\frac{x-\mu}{\sigma}\right)^2\right] dx, \qquad (18)$$

or

$$E(x) = \mu. \qquad (18a)$$

The variance of the normal distribution is

$$\text{Var}(x) = \sigma^2. \tag{19}$$

The two parameters of the normal distribution are the mean, μ, and the standard deviation, σ. The normal is symmetrical about the mean and is defined for values of x between positive infinity and negative infinity.

The cumulative density function of the normal distribution is given by

$$F(x) = \int_{-\infty}^{x} \frac{1}{\sigma\sqrt{2\pi}} \exp\left[-\tfrac{1}{2}\left(\frac{x-\mu}{\sigma}\right)^2\right]dx. \tag{20}$$

This integral can only be approximately evaluated. Tables of its values exist for $\mu = 0$ and $\sigma = 1$.

For normal distribution $\alpha_3 = 0$, which shows that the distribution is symmetrical, and $\alpha_4 = 3$ (7, pp. 123-124).

B. The Lognormal Distribution

A distribution closely associated with the normal is the lognormal. This is the distribution of a random variable whose logarithm follows the normal distribution. The lognormal probability density function is

$$f(x:\ \mu,\ \sigma) = \frac{1}{x\sigma''\sqrt{2\pi}} \exp\left[-\tfrac{1}{2}\,\frac{(\log x-\mu'')^2}{\sigma''^2}\right]. \tag{21}$$

x is defined from zero to positive infinity. The distribution is skewed to the right with skewness increasing as σ increases.

The mean of the lognormal is

$$\mu = e^{\mu''+\frac{1}{2}\sigma''^2}, \tag{22}$$

where

$$\mu'' = \frac{1}{n}\sum_{i=1}^{n} \log x_i, \tag{22a}$$

and

$$\sigma'' = \left[\frac{1}{n-1}\sum_{i=1}^{n} (\log x_i - \mu'')^2\right]^{\frac{1}{2}} \tag{22b}$$

and the variance is

$$\sigma^2 = e^{2\mu'' + \sigma''^2} (e^{\sigma''^2} - 1).$$

The coefficients of skewness and kurtosis are (7, pp. 127-128)

$$\alpha_3 = (e^{\sigma''^2} - 1)^{\frac{1}{2}} (e^{\sigma''^2} + 2), \tag{23}$$

and

$$\alpha_4 = 3 + (e^{\sigma''^2} - 1)(e^{3\sigma''^2} + 3e^{2\sigma''^2} + 6e^{\sigma''^2} + 6). \tag{24}$$

C. The Gamma Distribution

The gamma distribution is useful for representing the distribution of quantities which cannot be negative. It is appropriate to define the distribution of the times required for a total of exactly β independent events to take place if they occur at a constant rate η. It could be used to represent times-to-failure of components if the subcomponents fail independently with a constant rate η.

The gamma probability density function is

$$f(x: \beta, \eta) = \frac{\eta^{\beta}}{\Gamma(\beta)} x^{\beta-1} e^{-\eta x}. \tag{25}$$

It is defined for $x \geq 0$, $\beta > 0$, and $\eta > 0$. $\Gamma(\beta)$ is the gamma function.

The cumulative distribution of the gamma is

$$F(x: \beta, \eta) = \frac{\eta^{\beta}}{\Gamma(\beta)} \int_0^x x^{\beta-1} e^{-\eta x} \, dx. \tag{26}$$

The gamma distribution has a wide variety of shapes, and this accounts for much of the use of the model.

The mean is

$$\mu = \frac{\beta}{\eta}, \tag{27}$$

and the variance is

D. [illegible]

$$\sigma^2 = \frac{\beta}{\eta^2} . \tag{28}$$

[illegible]

The coefficients of skewness and kurtosis are (7, pp. 123-120).

$$\alpha_3 = \frac{2}{\sqrt{\beta}} ,$$

and

$$\alpha_4 = \frac{3(\beta + 2)}{\beta} .$$

D. The Erlangian Distribution

If η is restricted to positive integers, the gamma distribution is referred to as the Erlangian distribution. The distribution is sometimes more realistic in this form, as for most applications the fraction of an event has no meaning (7, p. 90).

E. The Exponential Distribution

The exponential distribution is often used as a times-to-failure distribution. It is used when the failure rate is assumed to be constant. It is the times-to-failure distribution if these failures are independent and happen at a constant average rate.

The probability density function for the exponential distribution is (7, pp. 123-124)

$$f(x:\eta) = \eta e^{-\eta x}, \tag{29}$$

and is defined for $x \geq 0$ and $\eta > 0$. The mean is

$$\mu = \int_0^\infty x\eta e^{-\eta x} dx \tag{30}$$

or

$$\mu = \frac{1}{\eta}. \tag{30a}$$

The variance is

$$\sigma^2 = \frac{1}{\eta^2}. \tag{31}$$

The coefficient of skewness is

$$\alpha_3 = 2, \tag{32}$$

and the coefficient of kurtosis is

$$\alpha_4 = 9. \tag{33}$$

From the values of α_3 and α_4 it is seen that the exponential distribution is skewed to the right and more peaked than the normal.

F. The Extreme-Value Distributions

The extreme-value distributions should be considered in a discussion of fatigue life distributions. In many applications the distribution of the largest or smallest elements of a sample are of interest. In failure analysis the distribution of the weakest components (smallest values) would be of interest. A distribution of the minimum of n independent values from a parent distribution that is unbounded to the left and is of exponential decreasing type is an extreme-value distribution. This distribution is the Type I for minimum values.

In reality, failure times cannot be negative. Therefore, the real life distributions of times-to-failure should be bounded by zero on the left. One such extreme-value distribution is the Weibull, referred to as the Type III extreme-value distribution.

G. The Weibull Distribution

The only distribution that was actually devised for use with fatigue data is the Weibull. It is an extreme value distribution of the smallest values. Using the Weibull to represent the breaking strength of a material has also been justified by Freudenthal and Gumbel (9).

The probability density function for the Weibull is (7, pp. 131-132)

$$f(x : \beta, \eta, \gamma) = \frac{\beta}{\eta}\left[\frac{x - \gamma}{\eta}\right]^{\beta-1} \exp\left[-\left[\frac{x - \gamma}{\eta}\right]^{\beta}\right]. \qquad (34)$$

$\beta > 0$ is the shape parameter.

$\gamma \geq 0$ is the location parameter.

$\eta > 0$ is the scale parameter.

The mean of the function is (11, pp. 2-15)

$$\mu = \gamma + \eta\,\Gamma\left[\frac{1}{\beta} + 1\right]. \qquad (35)$$

The variance is (7, p. 132)

$$\sigma^2 = \eta^2\left[\Gamma\left[\frac{2}{\beta} + 1\right] - \Gamma^2\left[\frac{1}{\beta} + 1\right]\right]. \qquad (36)$$

The coefficient of skewness is (7, p. 132)

$$\alpha_3 = \frac{\Gamma(1 + 3/\beta) - 3\Gamma(1 + 2/\beta)\,\Gamma(1 + 1/\beta) + 2[\Gamma(1 + 1/\beta)]^3}{\{\Gamma(1 + 2/\beta) - [\Gamma(1 + 1/\beta)]^2\}^{3/2}} \qquad (37)$$

and the coefficient of kurtosis is (7, p. 132)

$$\alpha_4 = \frac{\Gamma(1+4/\beta)-4\Gamma(1+3/\beta)[\Gamma(1+1/\beta)]+6\Gamma(1+2/\beta)[\Gamma(1+1/\beta)]^2-3[\Gamma(1+1/\beta)]^4}{\{\Gamma(1+2/\beta) - [\Gamma(1+1/\beta)]^2\}^2} . \quad (38)$$

The cumulative distribution function is given by

$$F(x) = 1 - \exp\left[-\left(\frac{x-\gamma}{\eta}\right)^{\beta}\right]. \quad (39)$$

This is the unreliability function. The reliability function is defined as

$$R(x) = 1 - F(x), \quad (40)$$

or

$$R(x) = \exp\left[-\left(\frac{x-\gamma}{\eta}\right)^{\beta}\right], \quad (40a)$$

and

$$\frac{1}{R(x)} = \exp\left[\left(\frac{x-\gamma}{\eta}\right)^{\beta}\right]. \quad (40b)$$

If the location parameter is zero,

$$\frac{1}{R(x)} = \exp\left(\frac{x}{\eta}\right)^{\beta},$$

then

$$\log\left(\frac{1}{R(x)}\right) = \left(\frac{x}{\eta}\right)^{\beta}$$

and

$$\log\log\left(\frac{1}{R(x)}\right) = \beta \log x - \beta \log \eta. \quad (40c)$$

This equation is of the form

$$Y = AX + B$$

with $$Y = \log \log \left\{ \frac{1}{R(x)} \right\}$$

and $$X = \log x,$$

$$B = -\beta \log \eta \qquad (41)$$

Using Weibull probability paper and plotting the times-to-failure results, it can be determined if the Weibull distribution describes the data. If a straight line fits the plotted points, then the Weibull distribution is sufficient for describing the data. In addition, the parameters of the distribution can be determined from this plot. The slope of the line is β, the shape parameter. η is the abscissa corresponding to an ordinate value of 63.2 percent on the Weibull plot. If a straight line fits the plotted data points, then $\gamma = 0$. If not, and a curve drawn through the points exhibits a concave downward behavior, then the data may be adjusted so that a straight line fits them satisfactorily. Then the value of γ can be determined, by the method given by Lochner (18).

H. The Beta Distribution

The beta distribution is useful to describe variations over a finite range. It has limited use for predicting cycles-to-failure but is included here for completeness. The beta probability density function is (7, pp. 127-128)

$$f(x:\ \beta,\ \eta) = \frac{\Gamma(\beta + \eta)}{\Gamma(\beta)\ \Gamma(\eta)}\, x^{\eta-1}(1 - x)^{\beta-1} \tag{42}$$

for x defined over the interval zero to one, and η and $\gamma > 0$. The mean is

$$\mu = \frac{\eta}{\beta + \eta}\ . \tag{43}$$

The variance is

$$\sigma^2 = \frac{\beta\ \eta}{(\beta + \eta)^2\ (\beta + \eta + 1)}\ . \tag{44}$$

The coefficient of skewness is

$$\alpha_3 = \frac{2(\beta - \eta)\ (\eta + \beta + 1)^{1/2}}{(\beta\eta)^{1/2}\ (\eta + \beta + 2)}\ . \tag{45}$$

The coefficient of kurtosis is

$$\alpha_4 = \frac{3(\beta + \eta + 1)\ [2(\eta + \beta)^2 + \beta\eta(\beta + \eta - 6)]}{\beta\eta(\beta + \eta + 2)\ (\beta + \eta + 3)}\ . \tag{46}$$

V THEORIES OF FATIGUE FAILURE AND THE DISTRIBUTIONS ASSOCIATED WITH THESE THEORIES

In this section the three predominant theories of fatigue failure are discussed. Also an attempt is made to show how each one of these phenomenological theories leads to the use of a particular distribution.

Many tests have been performed on fatigue failure, and some characteristics have been observed. Beyond a certain number of cycles of operation the occurrence of fracture is probabilistic (10, p. 214). This number is stress dependent. Many cases show a positive skewness to the frequency distribution of fatigue life (10, p. 214). The scatter in fatigue life decreases as the stress is increased (10, pp. 214-215).

Fatigue life of a specimen can be divided into four (10, p. 218) stages. The first stage of n_1 cycles is the completion of work hardening. The second stage of n_2 cycles is the time in which the first microcracks are formed. The third stage of n_3 cycles is the period during which the submicrocracks grow and link to form a crack of detectable size. During the fourth stage of n_4 cycles these cracks propagate across grains until fracture or rupture occurs. The end of stage 3 and the beginning of stage 4 are not clearly defined, and the period between formation of a detectable crack and rupture is a small part of the total life. Therefore, the contributors to the scatter in fatigue life are the second and third stages.

It is the rate of crack growth which determines the number of cycles before failure after the first cracks have been formed. At low stress levels, just above endurance, cracks have been found to exist after 50% of fatigue life. At higher stress levels cracks appear just before failure (10, Figure 139, p. 208).

A. The Weakest Link Theory

The weakest link theory treats each component as a series of many subcomponents. It interprets the strength of the component in terms of the minimum values of the strengths of the subcomponents. Each link will have cracks with a certain distribution, and the component will fail when the weakest link fails.

The cracks or defects are distributed throughout the specimen. Of the n total subcomponents the least strong determines the strength. The distribution of interest will be that of the minimum values of the subcomponent strengths in n subcomponents. If the life cycles of the subcomponents have a probability density function, f(x), the cumulative distribution function, F(x), is the probability that the life cycles do not exceed x and is defined as

$$F(x) = \int_{-\infty}^{x} f(x)\, dx. \tag{47}$$

The life lengths of the aggregated component would be distributed according to the smallest order statistic; thus,

$$F_n(x) = 1 - [1 - F(x)]^n. \tag{48}$$

Consequently, the probability density function, $f_n(x)$, of the smallest value of the n life cycles is (11, p. 2-6)

$$f_n(x) = n[1 - F(x)]^{n-1} f(x). \tag{48a}$$

The Weibull distribution is a smallest value distribution. If the subcomponents have a life distribution of the Weibull form, then

$$F(x) = 1 - e^{-\left(\frac{x-\gamma}{\eta}\right)^{\beta}}, \tag{49}$$

and the cumulative distribution of the aggregate from Equation 48 becomes

$$F_n(x) = 1 - \exp\left[-n\left(\frac{x-\gamma}{\eta}\right)^{\beta}\right] \tag{50}$$

and the pdf is then given by (11, pp. 2-6)

where

$$f_n(x) = \frac{n\beta}{\eta}\left(\frac{x-\gamma}{\eta}\right)^{\beta-1} \exp\left[-n\left(\frac{x-\gamma}{\eta}\right)^{\beta}\right] \tag{51}$$

There are also other subcomponent populations which will lead to the Weibull distribution for the specimen if the weakest link theory is accepted. Fisher and Tippet (12) have shown that many distributions, including the normal, can have their smallest values distributed as an extreme-value distribution.

B. The Parallel Strand Theory

To understand this theory it is convenient to consider the strands of a multistranded rope. The component is made up of subcomponents such as the strands of a rope and cannot fail until every strand has failed. Life lengths of the subcomponents determine the life pattern of the component. The life pattern of the component is the convolution of the life patterns of the subcomponents.

If the subcomponents had life lengths that were independent and identically distributed, the life length for the component would be the n-fold convolution of the subcomponent distributions. If the subcomponents have a probability density function f(x), the life length pdf, g(x), of the component will be (11, pp. 2-7)

$$g(x) = [f(x)]^{n*} \tag{52}$$

where

$$[f(x)]^{n*} = [f(x)] *[f(x)]^{(n-1)*} \tag{53}$$

and

$$[f(x)]^{(n-1)*}=[f(x)] *[f(x)]^{(n-2)*} \tag{53a}$$

and

$$[f(x)]^{2*} = [f(x)] *[f(x)] \tag{54}$$

or

$$[f(x)]^{2*} = \int_{-\infty}^{\infty} f(t)\, f(x-t)\, dt \tag{54a}$$

Assume the life distributions of the parallel strands are exponentially distributed; then

$$f(x) = \eta e^{-\eta x} \tag{55}$$

and

$$[f(x)]^{2*} = \int_{0}^{x} \left(\eta e^{-\eta t}\right)\left(\eta e^{-\eta(x-t)}\right) dt \tag{56}$$

and

$$[f(x)]^{2*} = \eta^2 \int_{0}^{x} e^{-\eta x}\, dt \tag{56a}$$

or

$$[f(x)]^{2*} = \eta^2\, t\, e^{-\eta x} \Big|_{0}^{x} \tag{56b}$$

Therefore,

$$[f(x)]^{2*} = \eta^2 \, x \, e^{-\eta x}. \tag{56c}$$

Similarly,

$$[f(x)]^{3*} = \eta^3 \int_0^x t \, e^{-\eta t} \, e^{-\eta(x-t)} \, dt, \tag{57}$$

$$[f(x)]^{3*} = \frac{1}{2}\eta^3 \, x^2 \, e^{-\eta x}, \tag{57a}$$

and (11, pp. 2-7 and 2-8)

$$[f(x)]^{4*} = \frac{1}{3!} \eta^4 \, x^3 \, e^{-\eta x} \, . \tag{58}$$

Consequently,

$$[f(x)]^{n*} = \frac{1}{(n-1)!} \eta^n \, x^{n-1} \, e^{-\eta x}, \tag{59}$$

or

$$g_n(x) = [f(x)]^{\eta*} = \frac{\eta^n \, x^{n-1}}{\Gamma(n)} \, e^{-\eta x} \, . \tag{59a}$$

It is seen from Equation 59a that the pdf of the component is defined by a gamma distribution.

If the number of strands approaches infinity, as it would for a metal specimen, the life length distribution $g_n(x)$ approaches the

normal function. As the shape parameter of the distribution, η, increases, the gamma distribution tends to normality with a mean of n/η and a variance of n/η^2 (11, p. 2-8).

C. The Proportional Effect Theory

A component is assumed to fail when the size of a crack reduces the cross sectional area to a certain value. A crack propagates at an exponential rate. The crack length is proportional to the length of the preceeding stage. Assume the size of a fatigue crack at various stages of its growth can be represented by the sequence $x_1 < x_2 < \ldots x_r < \ldots < x_n$, where x_r is the size of the crack at the r^{th} stage. x_n is the size of the crack when the cross sectional area is reduced to a value that cannot sustain the applied stress, and rupture occurs. The crack growth $x_i - x_{i-1}$ at the i^{th} stage is proportional to the crack size x_{i-1} of the preceeding stage, or

$$x_i - x_{i-1} = \partial_i x_{i-1} \quad . \tag{60}$$

x_o can be interpreted to be the size of minute flaws in the original component. $\partial_1, \partial_2, \ldots$ are independently distributed proportionality constants (11, p. 2-8). Then

$$x_i = \partial_i x_{i-1} + x_{i-1}, \tag{60a}$$

and

$$x_i = x_{i-1}(\partial_i + 1). \tag{60b}$$

It follows that

$$x_{i-1} = x_{i-2}(\partial_{i-1} + 1), \tag{60c}$$

$$x_2 = x_1(\partial_2 + 1), \tag{60d}$$

$$x_1 = x_o(\partial_1 + 1). \tag{60e}$$

Then

$$x_2 = x_o(\partial_1+1)(\partial_2+1), \tag{61}$$

$$x_{i-1} = x_o(\partial_1+1)(\partial_2+1) \ldots (\partial_{i-1}+1), \tag{61a}$$

and

$$x_i = x_o(\partial_1+1)(\partial_2+1) \ldots (\partial_{i-1}+1)(\partial_i+1). \tag{61b}$$

The component is assumed to fail when the size of the crack reaches x_n. The characteristic life length of the component is the distribution of x_n, where

$$x_n = x_o(\partial_1+1)(\partial_2+1) \ldots (\partial_n+1). \tag{61c}$$

From Equation 61c it may be seen that x_n is the product of independently distributed random variables. The logarithm of x_n is the sum of independent random variables, or

$$\log x_n = \log x_o + \log (\partial_1+1) + \ldots + \log (\partial_n+1). \tag{62}$$

The central-limit theorem states that log x_n is approximately normally distributed if n is large. If log x_n is normally distributed, then x_n is lognormally distributed (11, p. 2-8).

At higher amplitudes of alternating stress many cracks are formed. The growth rate of each of these cracks follows the proportional-effect theory. However, the crack lengths interlink and cause a random reduction of component area. At lower stress levels only one crack usually exists. The growth of this single crack also follows the proportional-effect theory.

Freudenthal (13) proposes a derivation for the distribution of component failure using the proportional-effect theory. It is based on the assumption that a single crack is formed and it propagates to cause failure.

Let $c_1, c_2, \ldots, c_k$ be consecutive cycles applied to a specimen at a constant stress amplitude, and let the extent of damage done to the area M by the cycles $c_1, c_2, \ldots, c_k$ be M_k. The increase in the damage done by cycle c_k is $M_k - M_{k-1}$. This increase is proportional to the effect of the cycle c_{k-1} and is related by some function $\phi(M_k)$; consequently,

$$M_k - M_{k-1} = c_k \, \phi(M_k), \tag{63}$$

$$c_k = \frac{M_k - M_{k-1}}{\phi(M_k)}, \tag{64}$$

and

$$\sum_{k=1}^{n} c_k = \sum_{k=1}^{n} [(M_k - M_{k-1})/\phi(M_k)]. \tag{65}$$

If each cycle contributes only slightly to the disruption of the area, the sum can be replaced by

$$\sum_{k=1}^{n} c_k = \int_{M_o}^{M_n} \frac{dM}{\phi(M)} . \tag{66}$$

If the effect of each cycle is directly proportional to the extent of damage produced by the previous cycle, then $\phi(M)$ is constant, and

$$\sum_{k=1}^{n} c_k = \int_{M_o}^{M_n} \frac{dM}{kM} = k' \log M_n/M_o \tag{67}$$

where M_o is the extent of the initial damage.

The central limit theorem states that the sum of n independent ramdom variables tends toward a normal distribution as n increases. If the number of cycles is large, then $\log M_n/M_o$ is normally distributed.

Making the assumption that the average rate of damage is proportional to the damage produced by a given number of cycles and that the cycles to produce a given amount of damage is inversely proportional to the rate, the number of cycles to fracture is inversely proportional to M. The reciprocal transformation of the lognormal distribution is also lognormal, $\log x = - \log 1/x$. The distribution of fatigue life at a given stress level is, therefore, lognormal (10, pp. 235-236).

The derivation of Freudenthal, which shows the life length distribution of the component to be lognormal, explains the previously mentioned positive skewness of failure distributions. The interlinking

of cracks to cause random reduction in the cross sectional area at high stress levels indicates that these life length distributions are normal. This has been supported by our results and the results of other testing programs.

VI ANALYSIS OF THE FATIGUE RELIABILITY AND STATIC STRENGTH DATA GENERATED IN THIS RESEARCH

The decision as to which distribution should be chosen must be based on the plots of the cycles-to-failure and stress-to-failure data, and phenomenological reasoning. The data was generated on the three combined bending-torsion fatigue reliability research machines designed and built at The University of Arizona. The times-to-failure were determined to the nearest second by precision clocks* which started as soon as a test was underway and stopped when a micro-limit switch cut the power to the clock off as soon as the specimen failed. The time was then converted to cycles-to-failure using the rotational speed of the machines. The times-to-failure and their conversion to cycles-to-failure are given in Appendix A. The speed of the machines was calibrated to $\pm$ 5 rpm. The rotational speeds of the machines are:

Machine 1	1786 $\pm$ 5 rpm
Machine 2	1784 $\pm$ 5 rpm
Machine 3	1780 $\pm$ 5 rpm

For the data generated in this research and given in Tables 1, 2, and 3, it was decided to first plot the cycles-to-failure and stress-to-failure data on probability paper, study the results, correlate them with the previously discussed behaviors of the statistical distributions and the phenomenological aspects, and then draw conclusions as to which distribution best represents the data.

---

*Three stress levels of stress ratio ∞ were run with a positively driven revolution counter.

Based on the discussion of the distributions relevant to fatigue and static strength, it was decided to use only the normal, lognormal and Weibull distributions. Consequently, all of the cycles-to-failure data were plotted against median ranks (17, Table 1) on Weibull and lognormal probability paper for all stress levels of stress ratios ∞ and 0.70. The data for the two highest stress levels at each stress ratio were plotted against median ranks on normal probability paper also.

In Figure 5 are plotted the cycles-to-failure data for $r_s = \infty$ on Weibull probability paper. In Figure 6 are plotted the cycles-to-failure data for $r_s = \infty$ and s_a = 154,000 psi and 121,500 psi, on normal probability paper. In Figure 7 are plotted the cycles-to-failure data for $r_s = \infty$ and s_a = 154,000 psi, 121,500 psi, and 104,500 psi on lognormal probability paper. In Figure 8 are plotted the cycles-to-failure data for $r_s = \infty$ and s_a = 86,000 psi and 78,000 psi on lognormal probability paper.

In Figure 9 are plotted the cycles-to-failure data for r_s = 0.70 on Weibull probability paper. In Figure 10 are plotted the cycles-to-failure data for r_s = 0.70 and s_a = 110,500 psi and 97,500 psi on normal probability paper. In Figure 11 are plotted the cycles-to-failure data for r_s = 0.70 and s_a = 110,500 psi, 97,500 psi, 76,500 psi, and 70,000 psi on lognormal probability paper. Lastly, in Figure 12, are plotted the static tensile ultimate strength data for the notched specimens on normal probability paper.

In Figure 5, the data for the stress level of 154,000 psi plots concave upward. The location parameter, γ, could not be adjusted to give a better straight line fit (18, pp. 5-8). The raw data would lend themselves to a fairly good straight line fit at the stress levels of 121,500 psi, 104,500 psi, 86,000 psi, and 78,000 psi, if these lines were drawn. The lines on this Weibull probability paper were not drawn so that the raw data would stand out.

In Figure 6, the data for the stress level of 154,000 psi is concave upward indicating a distribution that is skewed to the left (16, p. 14). The data for the stress level of 121,500 psi gives a straight line fit with good correlation, as shown in Table 4, on normal paper.

Figures 7 and 8, and Table 4 show that the data for the stress levels of 121,500 psi, 104,500 psi, 86,000 psi, and 70,000 psi give straight line fits with good correlation on lognormal paper. A straight line can be fitted to the data for the stress level of 154,000 psi, although with not as good a correlation as at the other stress levels. The lack of an extremely good fit may be explained by the fact that only twelve data points are available at this stress level.

Figure 9, where the plots of the data for stress ratio of 0.70 are given on Weibull probability paper, shows that a straight line would fit the data at the lower stress levels of 76,000 psi and 70,000 psi with good correlation. The data for the higher stress levels of 110,500 psi and 97,500 psi, are concave downward. The adjustment of the location parameter did not yield a better straight line. The attempt to adjust for better fit was hampered by the lack of a larger number of data points.

Figure 10, where the data for the stress ratio of 0.70 are plotted on normal probability paper, indicates concave downward curves for the stress levels of 110,500 psi and 97,500 psi.

Figure 11 and Table 4 show good straight line fits at all stress levels for a stress ratio of 0.70 on lognormal probability paper.

In Figure 12 and Table 4, the ultimate strength data exhibit a good straight line characteristic on normal probability paper. The line has a steep slope indicating a narrow spread of the data. This is to be expected. Static strength distributions are usually normal. Juvinall (6, p. 351) states that static tests have a small statistical variation. Bompas-Smith (14, p. 344) also states that the probability density function of tensile tests can be expected to be normal.

Having described each figure, an overall analysis of each will be made in conjunction with the phenomenological aspects of fatigue, discussed previously. A straight line can be fitted to all the log-normal plots with fairly good correlation, as may be seen in Figures 7, 8, and 11, and Table 4. Phenomenologically, the acceptance of the proportional-effect theory, discussed earlier in this report, would result in the acceptance of the lognormal as the life length (cycles-to-failure) distribution of components subjected to fatigue. The conclusion that the characteristics of the lognormal distribution are associated with fatigue failures and that the lognormal is the failure governing distribution for fatigue is supported by both theory and experimental results.

Herd (19, p. 5) also reasons that the lognormal is an appropriate distribution for the cycles-to-failure data. He states that the lognormal distribution applies to situations in which several independent factors influence the outcome of an event, not additively, but according to the magnitude of the factor and the age of the item at the time the factor is applied. If the effect of each impulse is directly proportional to the momentary age, x, of the item, then log x would be normally distributed. Consequently, the x's would be log-normally distributed.

Yokobori (9, p. 194) states that a positive skewness to the distribution of fatigue life often exists, and the logarithms of cycles-to-failure can be approximated by a normal distribution. Results of tests that show the positive skewness are given by Yokobori (10, pp. 211 - 212). The derivation by Freudenthal (13) and the discussion of the proportional-effect theory (11, pp. 2-8) also result in the lognormal as the distribution of cycles-to-failure for fatigue. Bompas-Smith (14, p. 345) states that fatigue results at a constant stress level frequently conform to a lognormal distribution. F. Epremian and R. F. Mehl (15) suggest the values of the logarithms of cycles-to-failure are normally distributed about a

mean value. Juvinall (6, pp. 350-351) shows results of tests of fatigue life data that approximate the lognormal distribution.

Figure 10 shows curves that are concave downward. James R. King (16, p. 7) states that a concave plot on normal probability paper indicates a right-skewed distribution and that a logical choice would be the lognormal. Bompas-Smith (14, Figure 12, p. 349, and Figure 15, p. 350) confirms that a curve of this shape on normal probability paper gives rise to a straight line fit on lognormal probability paper.

Figure 9 indicates that the lognormal distribution would provide good fits at stress levels of 110,500 psi and 97,500 psi for the stress ratio of 0.70 because the curves are concave downward and Bompas-Smith (14, Figure 12, p. 349 and Figure 15, p. 350) shows that plots of this shape on Weibull probability paper give a straight line on lognormal probability paper.

The extreme-value function could phenomenologically be the life length distribution if only the weakest of the specimens were tested to failure. This does not completely describe the testing program by which this data was generated. The specimens to be tested were randomly selected and all were tested to failure. Although the Weibull plots show that a straight line fit to much of the data is plausible, it is in no case better than the straight line fit provided by the lognormal plots.

It is difficult with the eighteen data points at each stress level to determine the exact shape of the Weibull plots. It would be impossible to determine the shape with the five or seven data points recommended by King (16, p. 12). This is true for any other distribution. With only a few data points, no absolute statements can be made from the plots. That is why the plots must be used along with phenomenological reasoning to determine the failure governing distributions.

Phenomenological reasoning can also be used to justify the use of the normal as the failure distribution at the high stress, or low fatigue life, levels. Juvinall (6, p. 351) states that short life fatigue tests approach static test characteristics which have small statistical variations. Bompas-Smith (14, p. 344) states that if the strength of a component is a function of several variables, the failure distribution tends to normality. Yokobori (10, p. 215) states that the scatter of fatigue life increases as the stress level decreases. This is verified by the data in Tables 1 and 4, and Figures 6 and 10.

A computer program was written to fit the best straight line to the data (straight cycles-to-failure, and logarithms of the cycles-to-failure). This program uses the least squares method and fits the best straight line to the data for stress ratios ∞ and 0.70 on normal and lognormal plots. The program also fits the best straight line to the data for the stress ratio of 0 on the normal plot and computes the correlation coefficient.

The correlation coefficients for the data fits at the various stress levels differ only slightly between the normal and lognormal distributions. The maximum difference is 2.2%, as may be seen from Table 4. Basing the analysis on the relatively few data points makes it impossible to discriminate between the normal and the lognormal distributions solely on the basis of the correlation coefficient.

The straight line fit to the data for stress ratio 0 is very good, because a very high correlation coefficient was obtained. The coefficients of correlation and the equations of the best straight lines are given in Table 4. Phenomenological reasoning, experimental results and graphical analysis dictate that the normal distribution should best describe the stress-to-failure data a stress ratio of 0.

Although in many cases the straight line fit to the data on normal probability paper gives a higher correlation coefficient, the lognormal has been chosen to represent the cycles-to-failure

distribution. The small sample size used in this research has not provided sufficient opportunity for significant discrimination between the normal and the lognormal distributions. Furthermore, the lognormal distribution has been phenomenologically justified and is seen to better represent the data, when all stress levels are considered, than any other applicable distribution discussed in this report.

VII CONCLUSIONS

1. The Weibull distribution fit to the cycles-to-failure data at various stress levels (Figures 5 and 9) shows that the distribution might approximate the cycles-to-failure distribution of the specimens; however, the data points do not appear to lend themselves to a good straight line fit because of the kinks in the plot. Statistically, the Weibull distribution is an extreme-value distribution and does not describe the type of data generated in this research program.

2. The normal distribution fit to the cycles-to-failure data at the various stress levels for the stress ratio of ∞ and 0.70 (Figures 6 and 10, and Table 4) shows that the normal distribution might represent the cycles-to-failure distributions of the specimens, because there is good straight line fit and there is no significant difference between the correlation coefficients for the normal and the next appropriate distribution, the lognormal. Phenomenologically, the normal distribution can be justified to approximate the cycles-to-failure distribution at the highest stress levels only.

3. The lognormal distribution fit to the cycles-to-failure data (Figures 7, 8, and 11, and Table 4) is good at all stress levels for stress ratios of ∞ and 0.70. The lognormal distribution phenomenologically describes the cycles-to-failure distributions of the specimens best at all stress levels.

4. Phenomenologically, statistically and probabilistic-graphically the normal distribution gives the best fit to the static ultimate strength data for the stress ratio of 0 (Figure 12 and Table 4). The straight line fits the data on normal probability paper with good correlation and has a steep slope showing a small dispersion.

5. The difficulty of discriminating between the normal and lognormal distribution fits to the cycles-to-failure data is attributed to the small sample size; namely, 12 specimens at the highest stress levels and 18 specimens at the other stress levels. It would be of great interest to see the degree of discrimination achieved when sample sizes of 50 or more are tested at each stress level.

6. The fact that the correlation coefficients for the straight line fits to the static ultimate strength data for notched specimens on the normal and the lognormal bases have no significant difference (Table 4) may again be attributed to the small sample size tested, namely 10.

7. The phenomenological reasoning leads to the conclusion that, were the cycles-to-failure data those of field failures or only of the failures from a larger sample, all of which were not tested to failure, the Weibull distribution would be the most appropriate distribution to represent such data. The primary reason for this is that such data would be the failures of the weakest of such components in field operation or in test, consequently, conforming to the extreme-value distribution theory. The cycles-to-failure data generated in this research are those of the whole sample being tested to failure; therefore, the data is that of the weakest, as well as, of the strongest specimens failing, hence not conforming to the extreme-value theory represented by the Weibull distribution.

8. Phenomenological reasoning leads to the conclusion that the cycles-to-failure data at all stress levels would be best represented by the lognormal distribution, and, except at the highest alternating bending stress levels, the lognormal distribution should be used exclusively for the cycles-to-failure data of the type generated in this research.

9. Phenomenological reasoning also leads to the conclusion that at the highest alternating bending stress levels, the normal distribution can be used to approximate the lognormal distribution. This provides a computational advantage when calculating the reliability

of a component by the design-by-reliability methodology.

10. A conclusion of caution is in order when attempts are made to apply the previous conclusions to test conditions not identical, or closely related, to those used in the generation of the data for this research. More complex test and field loadings will cause failures not represented by any one of the following idealized theories: he weakest link theory, the parallel strand theory and the proportional effect theory. Under these conditions some combination of these theories would be in effect. The cycles or times-to-failure data would then exhibit complex behavior not representable by any one distribution discussed in this report.

VIII RECOMMENDATIONS

1. There is not enough statistical evidence to discriminate between the normal and the lognormal at most stress levels. This is the result of testing 12 or 18 specimens at each stress level. and reflects the need to test more specimens at each stress level: preferably 50 or more.

2. A test program should be initiated to test the weakest components of a population and examine the cycles-to-failure behavior using the extreme-value distributions. These life length distributions would be of interest to design engineers because it is the weakest parts that fail in actual service.

3. Research of the type leading to this and the previous three reports should be continued to acquire the vast data needed for the effective application of the design-by-reliability methodology.

4. Statistical distributions which may represent the more complex test,or field, loading situations should be developed and studied.

ACKNOWLEDGMENTS

The contributions of the following people to this effort are gratefully acknowledged:

1. Mr. Vincent R. Lalli, NASA Project Manager.

2. Messrs. Jeffrey McConnell, John L. Smith, and Scott Clemans, all of The University of Arizona.

REFERENCES

1. "A Probabilistic Method of Designing Specified Reliabilities Into Mechanical Components with Time Dependent Stress and Strength Distributions," Dimitri Kececioglu, J. W. McKinley and Maurice J. Saroni, Report to NASA on Grant NGR 03-002-044, January 25, 1967, 331 pp.

2. "Design and Development of and Results From Combined Bending-Torsion Fatigue Reliability Research Machines," D. B. Kececioglu, M. J. Saroni, H. Wilson Broome, and Jeffrey McConnell, Report to NASA on Grant NGR 03-002-044, July 15, 1969, 57 pp.

3. "A Method for Obtaining and Analyzing Sensitivity Data," W. J. Dixon and A. M. Mood, Journal of the American Statistical Association, Volume 43, 1948, pp. 109-126.

4. "Thermal Stress and Low-Cycle Fatigue," S. S. Manson, McGraw-Hill Book Co., Inc., New York, 1966, 404 pp.

5. "Mechanical Engineering Design," J. E. Shigley, McGraw-Hill Book Co., Inc., New York, 1963, 631 pp.

6. "Stress, Strain and Strength," R. C. Juvinall, McGraw-Hill Book Co., Inc., New York, 1967, 580 pp.

7. "Statistical Methods in Engineering," G. J. Hahn and S. S. Shapiro, John Wiley and Sons, New York, 1967, 355 pp.

8. "Statistics and Experimental Design," Volume I, N. L. Johnson and F. C. Leone, John Wiley and Sons, 1964, 523 pp.

9. "On the Statistical Interpretation of Fatigue Tests," A. M. Freudenthal and E. J. Gumbel, Proceedings of the Royal Society, Great Britain, Vol. 216A, 1953, p. 309.

10. "Strength, Fracture, and Fatigue of Materials," Takeo Yokobori, P. Noordhoff, Groningen, The Netherlands, 1965, 372 pp.

11. "Reliability Handbook," W. Grant Ireson, Editor-in-Chief, McGraw-Hill Book Co., Inc., New York, 1966, 694 pp.

12. "Limiting Forms of the Frequency Distributions of the Largest or Smallest Member of a Sample," R. A. Fisher and L. H. C. Tippett, Proc. Cambridge Phil. Soc., Great Britain, Vol. 24, Part 2, 1928, p. 180.

13. "Symposium on Statistical Aspects of Fatigue," A. M. Freudenthal, ASTM, Special Technical Publication No. 121, 1952, p. 7.

14. "The Determination of Distributions that Describe the Failures of Mechanical Components," J. H. Bompas-Smith, 1969 Annals of Assurance Sciences, Eighth Reliability and Maintainability Conference , Denver, Colorado, July 7-9, 1969, Gordon and Breach Science Publishers, New York, 1969, 580 pp. 343 - 356.

15. "Investigation of Statistical Nature of Fatigue Properties," F. Epremian and R. F. Mehl, NACA TN 2719, June 1952.

16. "Graphical Data Analysis with Probability Papers," J. R. King, TEAM, Special Purpose Graph Papers, 104 Belrose Ave., Lowell, Mass., 1966, 17 pp.

17. "Theory and Techniques of Variation Research," L. G. Johnson, Elsevier Publishing Company, Amsterdam, 1964, 105 pp.

18. "When and How to Use the Weibull Distribution," R. H. Lochner, Lecture Notes of the Sixth Annual Reliability Engineering and Management Institute, The University of Arizona, Tucson, Arizona, October 9, 1963, 45 pp.

19. "Uses and Misuses of Distributions," Ronald B. Herd, Kaman Aircraft Corporation, Bethesda, Maryland, Proceedings Reliability Symposium, 1961, 7 pp.

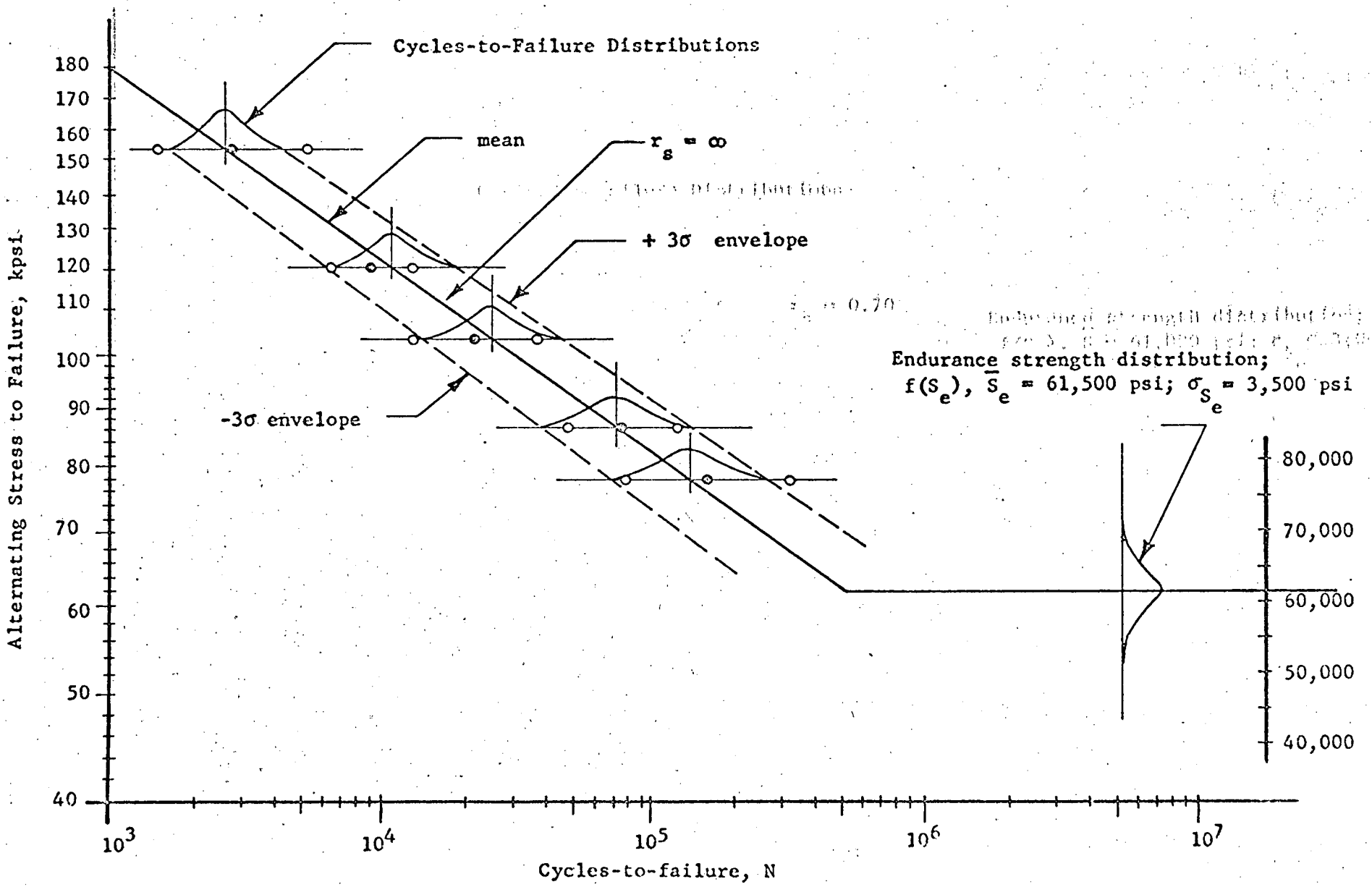

FIGURE 1. CYCLES-TO-FAILURE DISTRIBUTIONS AND ENDURANCE STRENGTH DISTRIBUTION FOR STRESS RATIO OF ∞.

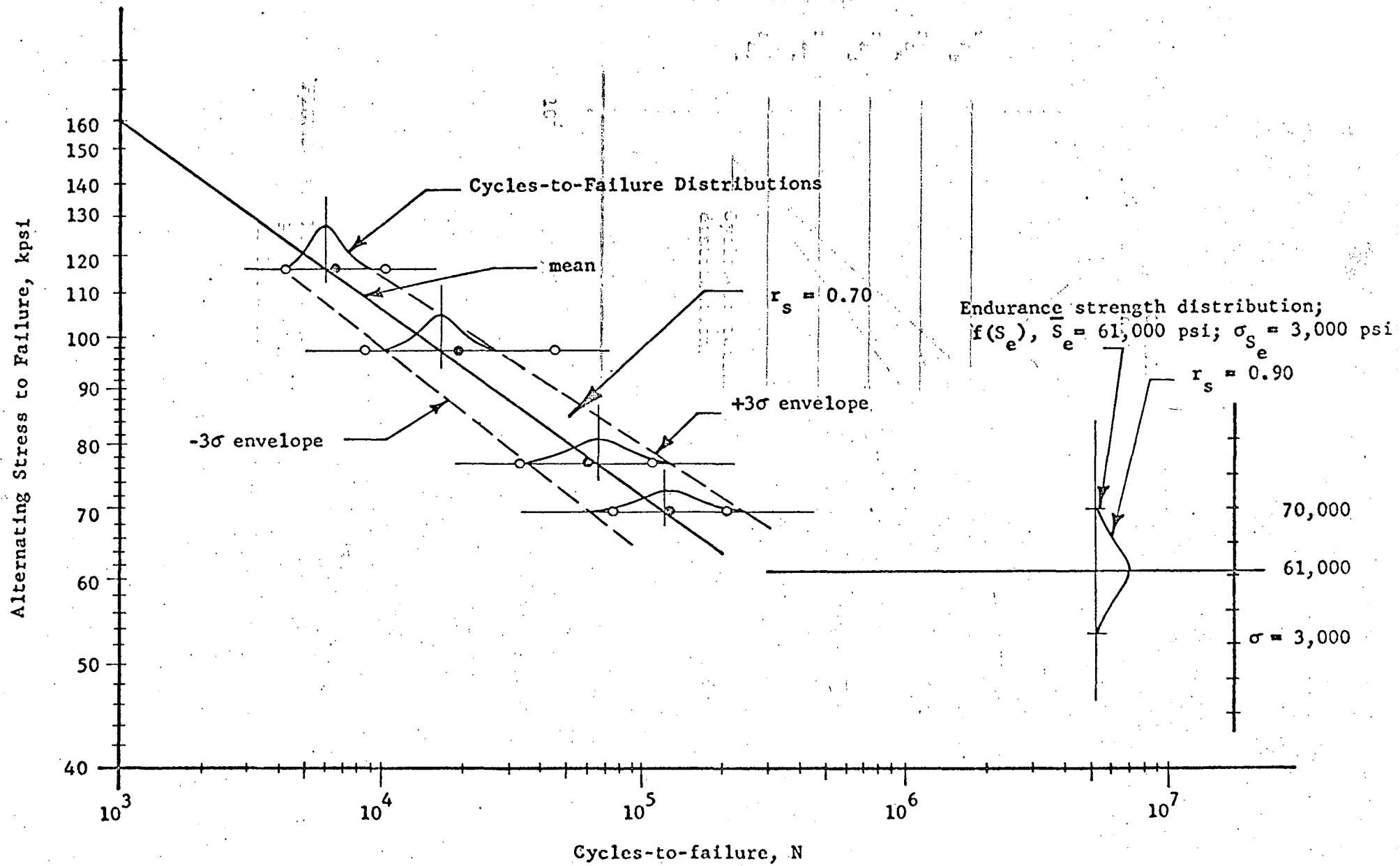

FIGURE 2. CYCLES-TO-FAILURE DISTRIBUTIONS FOR A STRESS RATIO OF 0.70 AND ENDURANCE STRENGTH DISTRIBUTION FOR A STRESS RATIO OF 0.90.

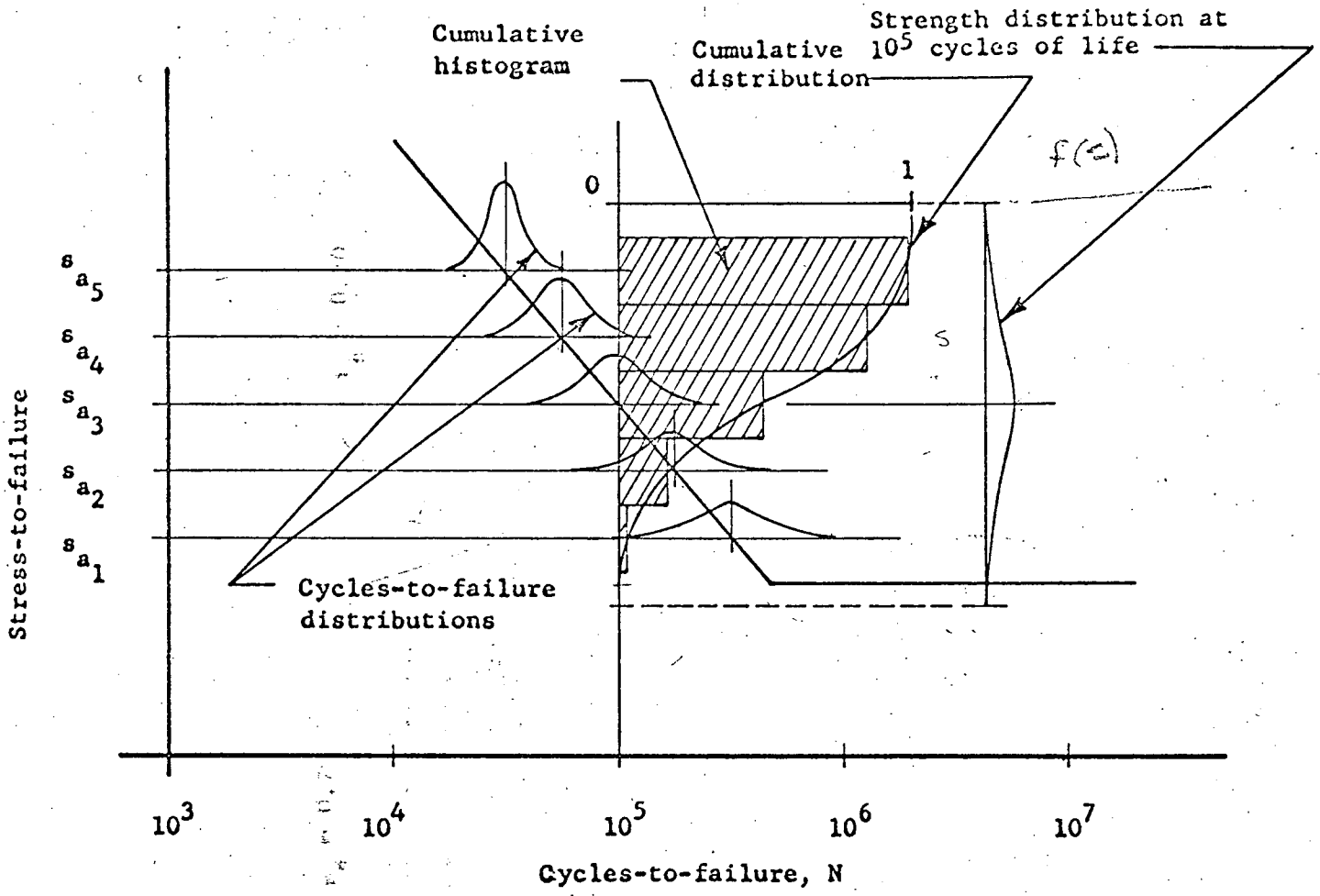

FIGURE 3. DISTRIBUTIONS OF THE CYCLES-TO-FAILURE AND STRESS-TO-FAILURE AT A SPECIFIC LIFE (10^5 CYCLES IN THIS EXAMPLE) AS FOUND BY FATIGUE TESTS AT A CONSTANT STRESS RATIO.

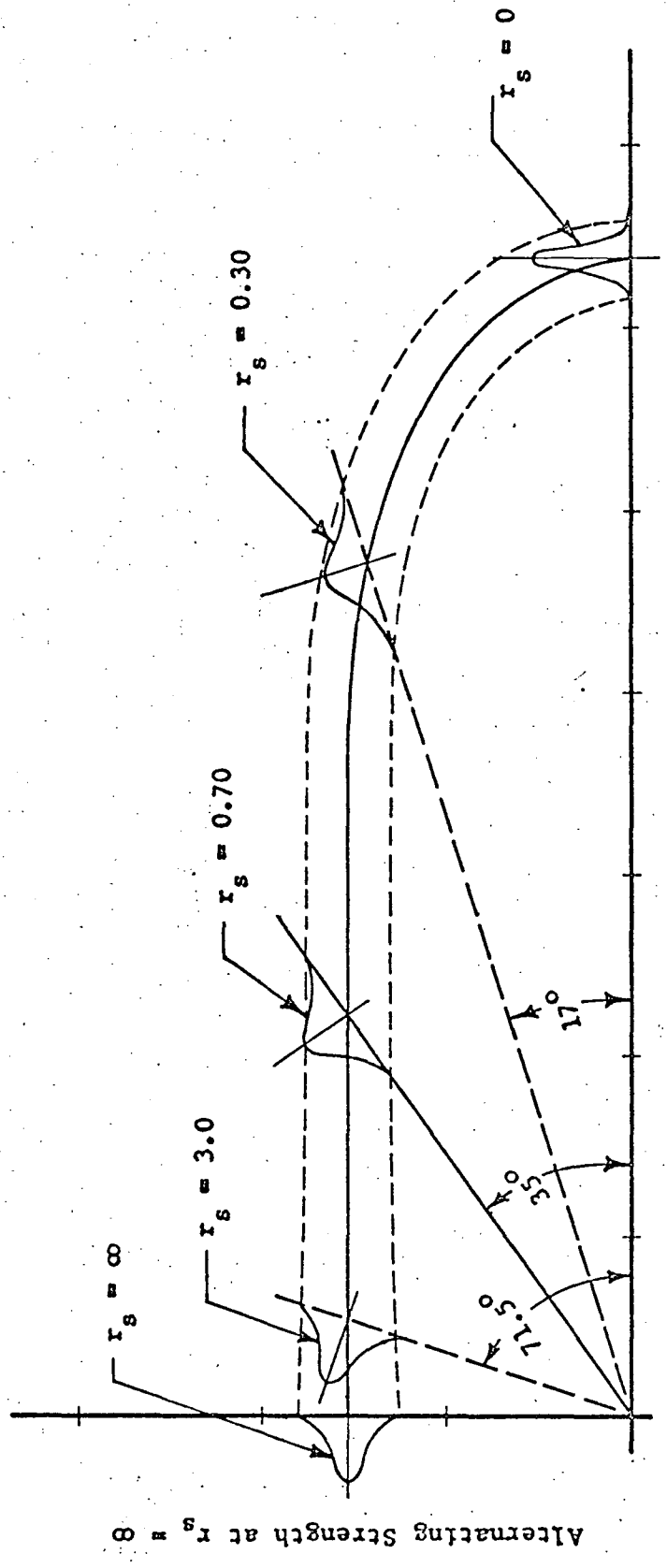

FIGURE 4. THREE-DIMENSIONAL, DISTRIBUTIONAL GOODMAN FATIGUE STRENGTH SURFACE FOR A SPECIFIED CYCLES OF LIFE.

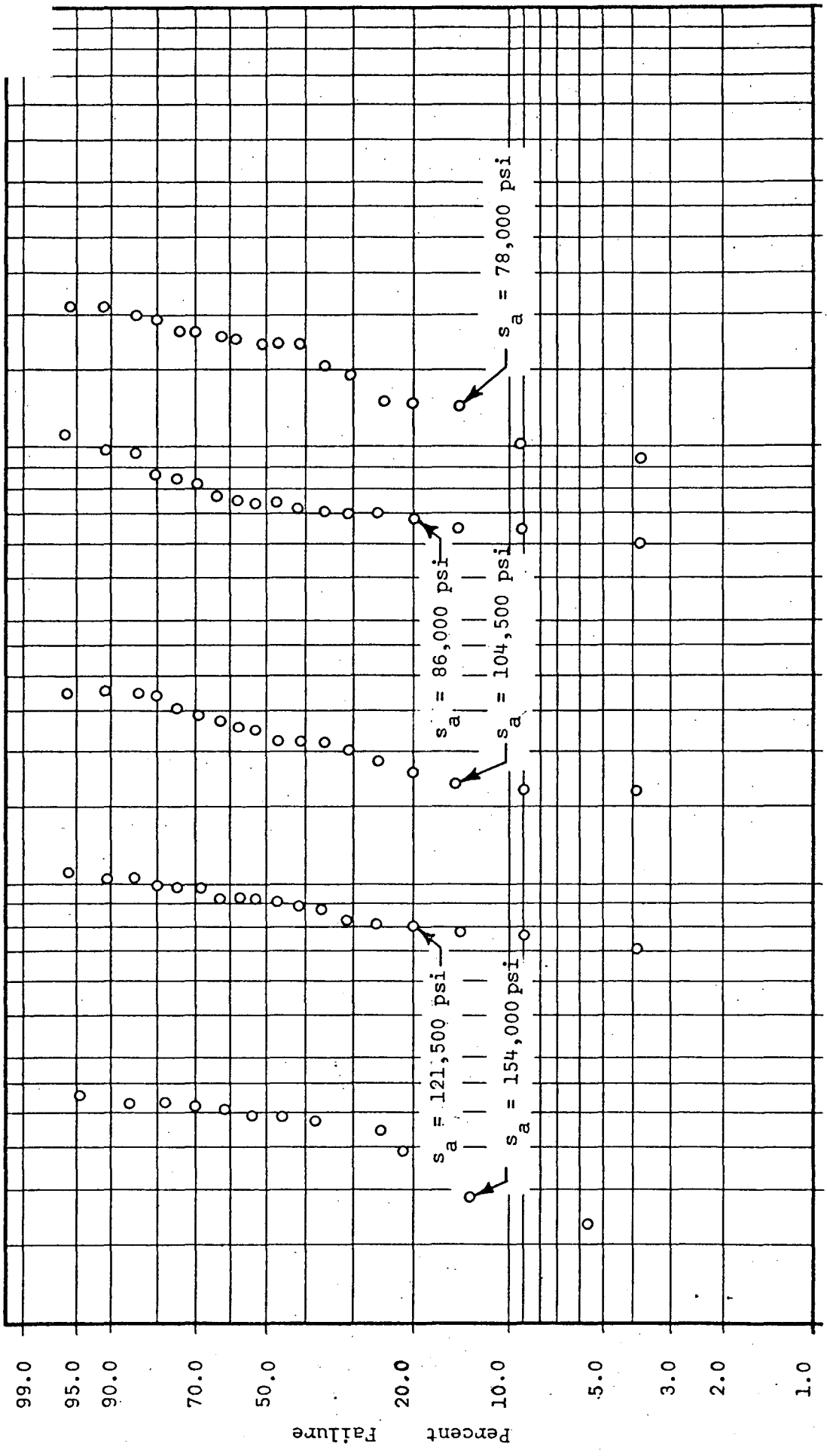

FIGURE 5. CYCLES-TO-FAILURE DATA FOR STRESS RATIO OF ∞ PLOTTED ON WEIBULL PROBABILITY PAPER.

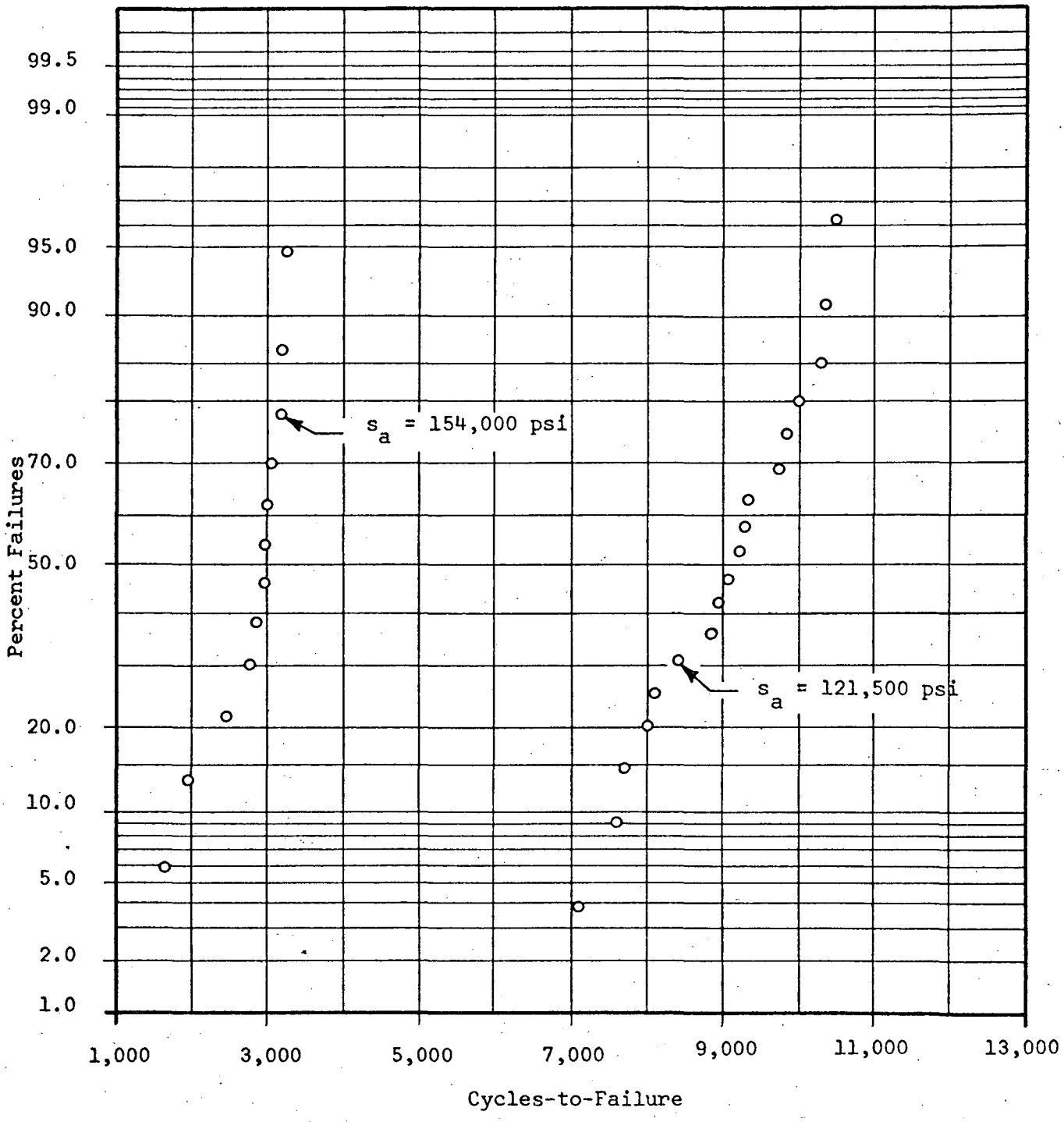

FIGURE 6. CYCLES-TO-FAILURE DATA FOR BENDING STRESSES OF 154,000 PSI AND 121,500 PSI AT STRESS RATIO OF ∞ PLOTTED ON NORMAL PROBABILITY PAPER.

F

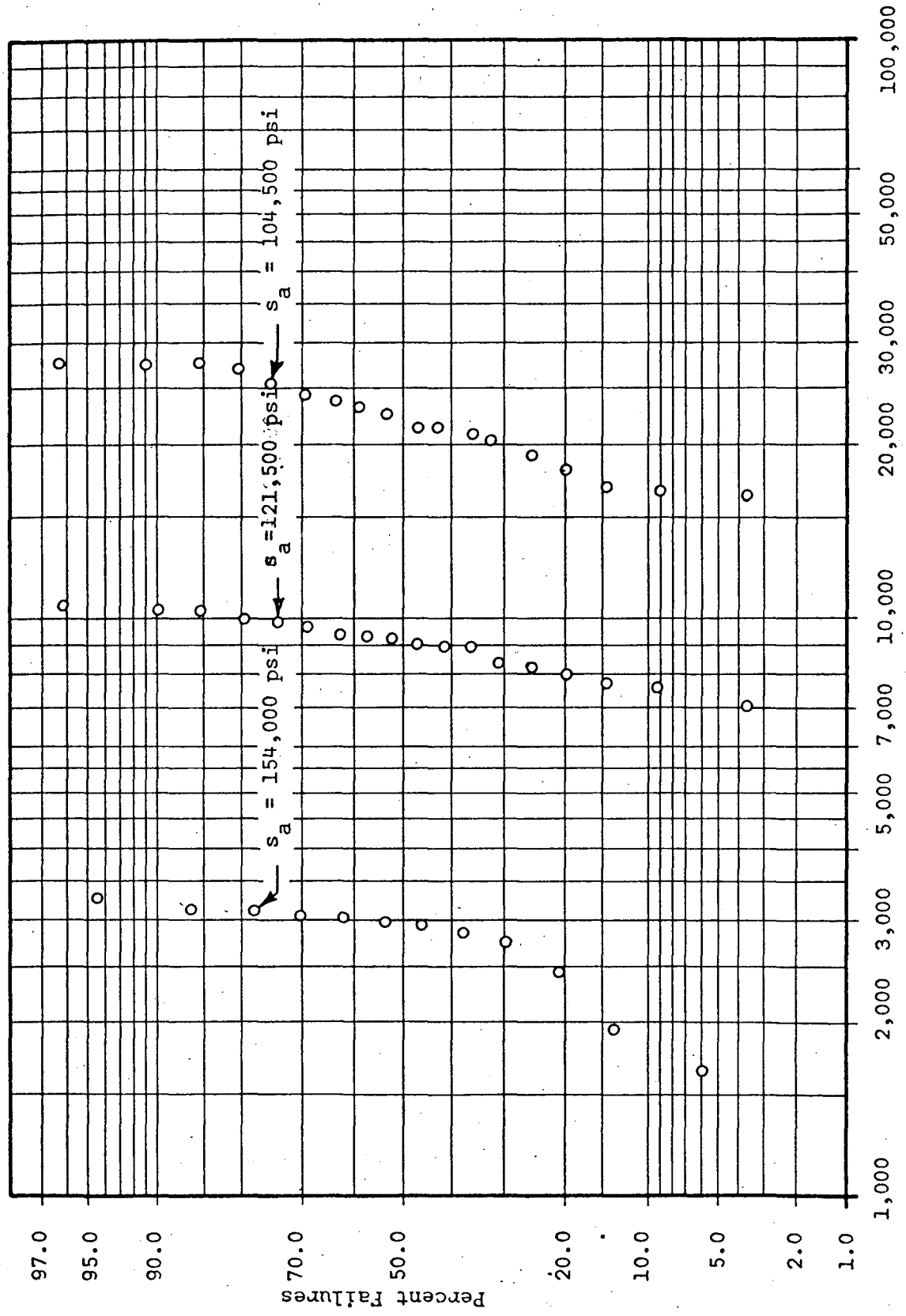

FIGURE 7. CYCLES-TO-FAILURE DATA FOR BENDING STRESSES OF 154,000 PSI, 121,500 PSI, AND 104,500 PSI AT STRESS RATIO OF ∞ PLOTTED ON LOGNORMAL PROBABILITY PAPER.

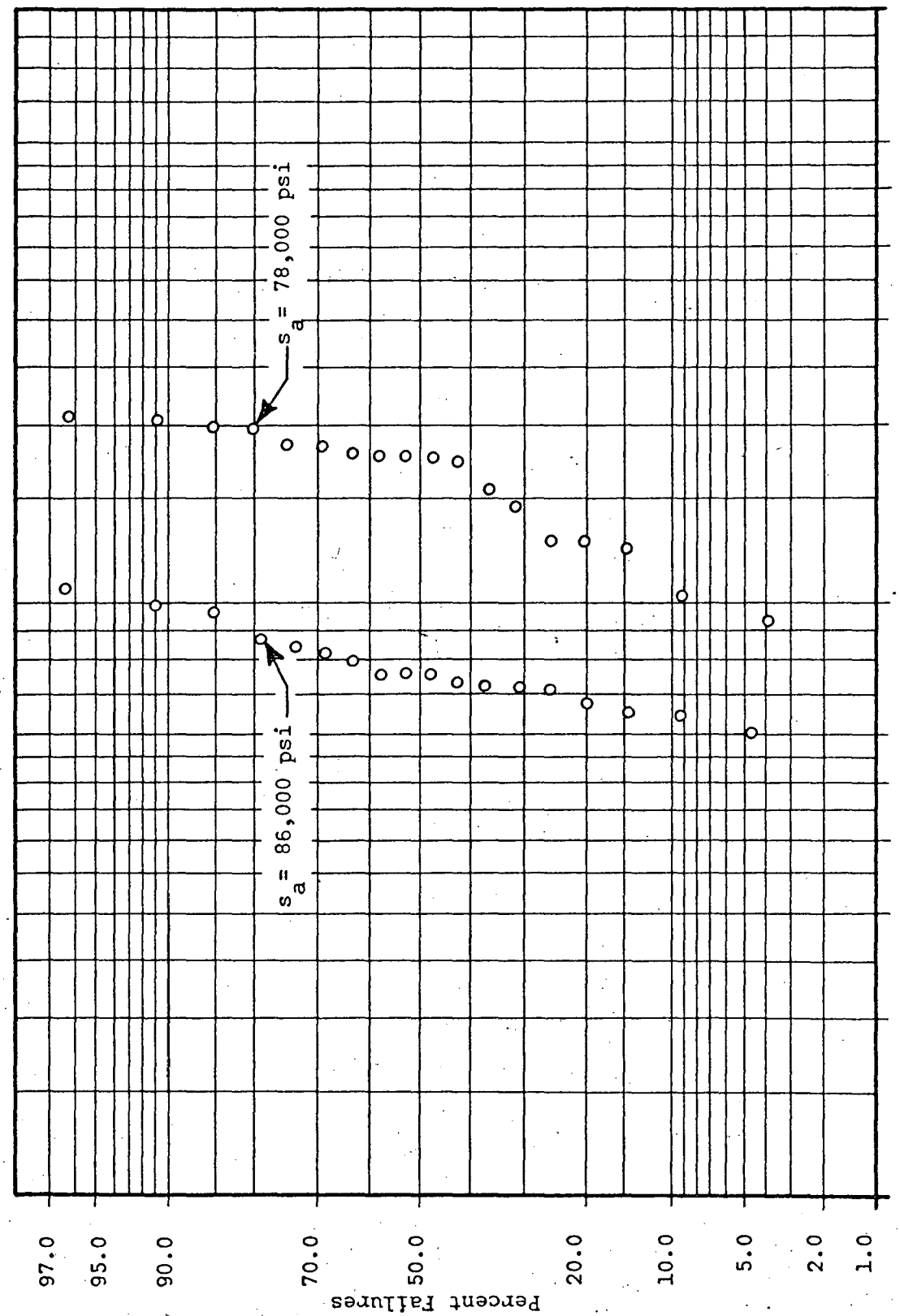

FIGURE 8. CYCLES-TO-FAILURE DATA FOR BENDING STRESSES OF 86,000 PSI AND 78,000 PSI AT STRESS RATIO OF ∞ PLOTTED ON LOGNORMAL PROBABILITY PAPER.

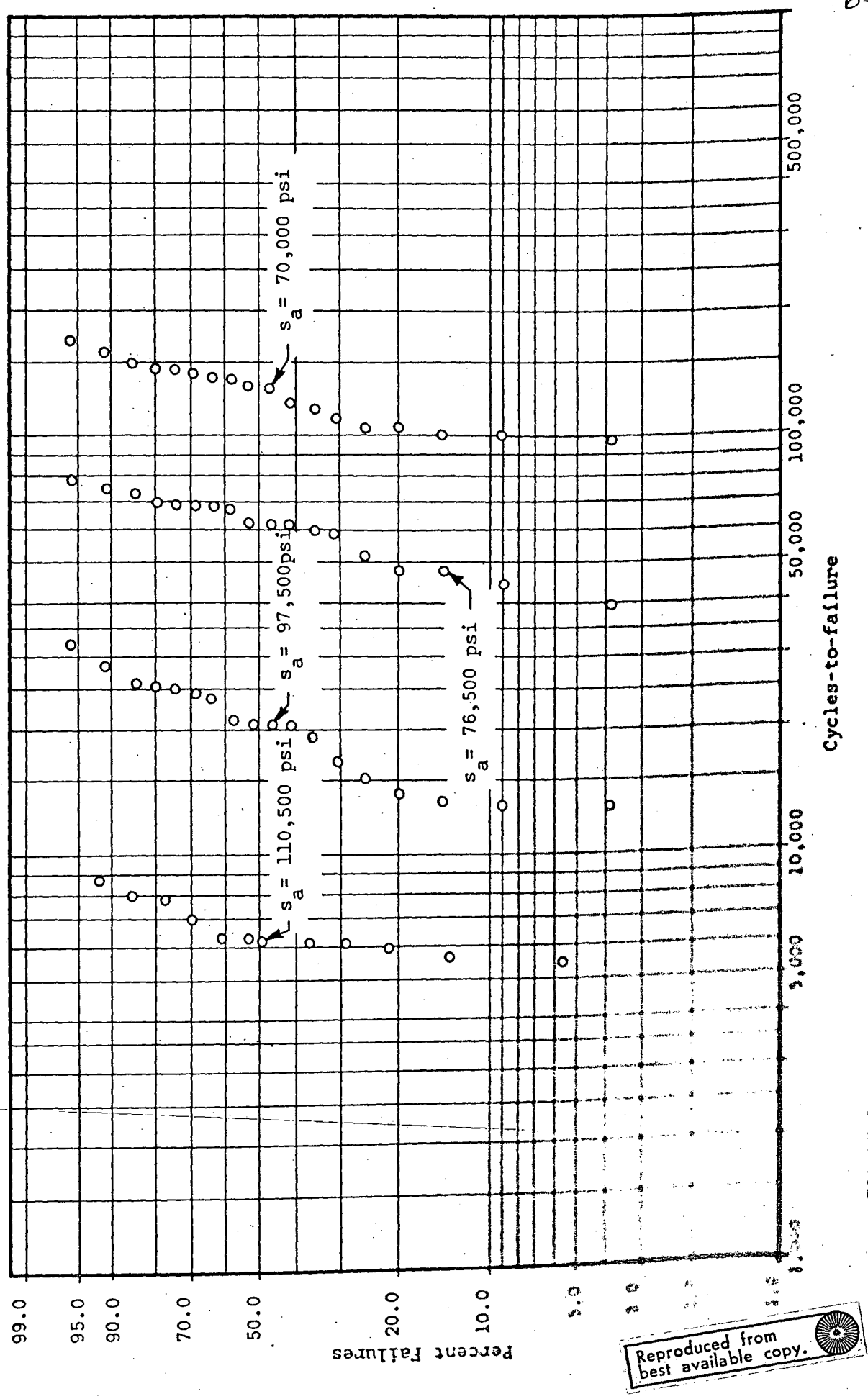

FIGURE 2. CYCLES-TO-FAILURE DATA FOR STRESS RATIO OF 0.70 PLOTTED ON WEIBULL PROBABILITY PAPER.

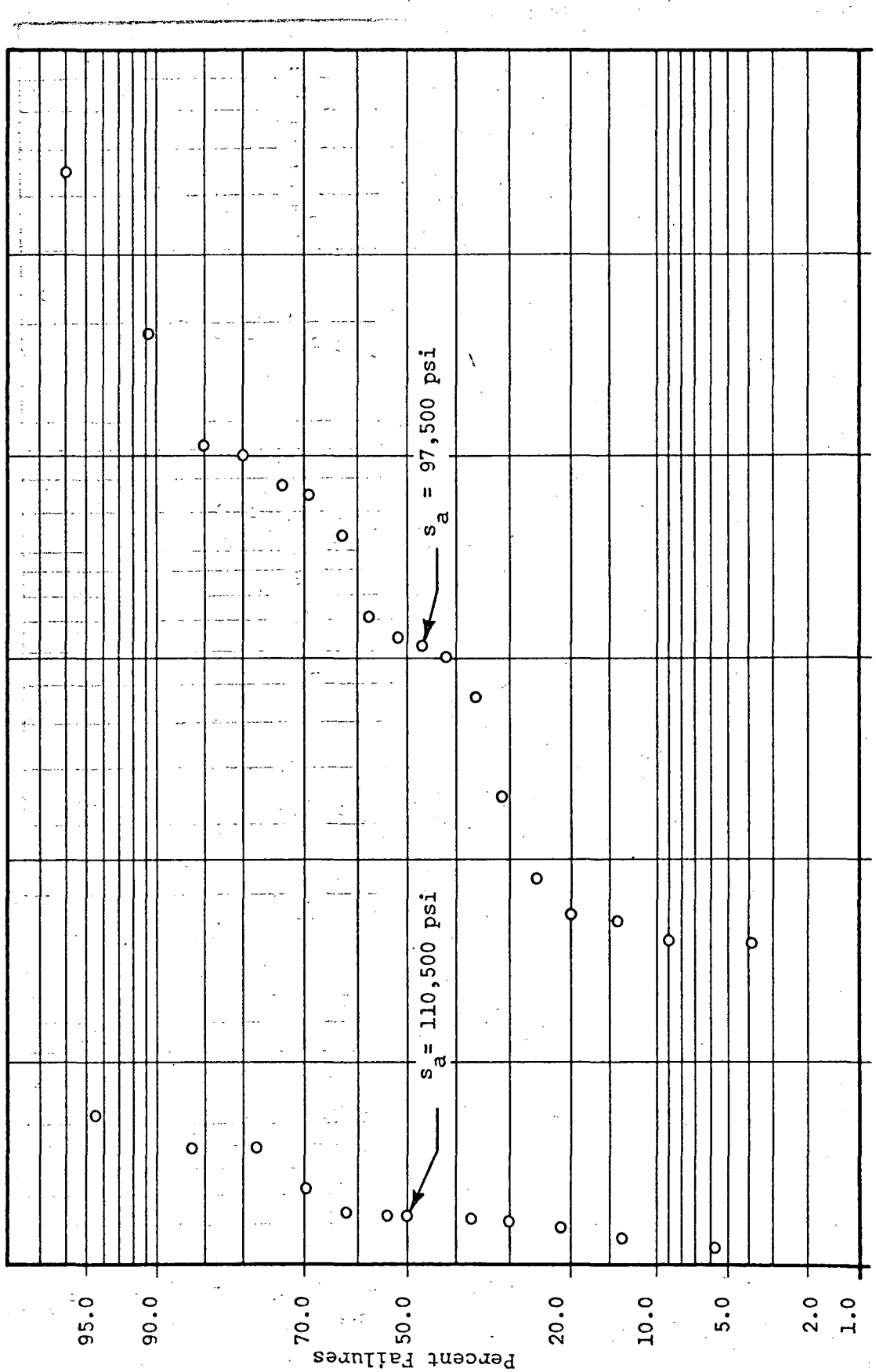

FIGURE 10. CYCLES-TO-FAILURE DATA FOR BENDING STRESSES OF 110,500 PSI AND 97,500 PSI AT A STRESS RATIO OF 0.70 PLOTTED ON NORMAL PROBABILITY PAPER.

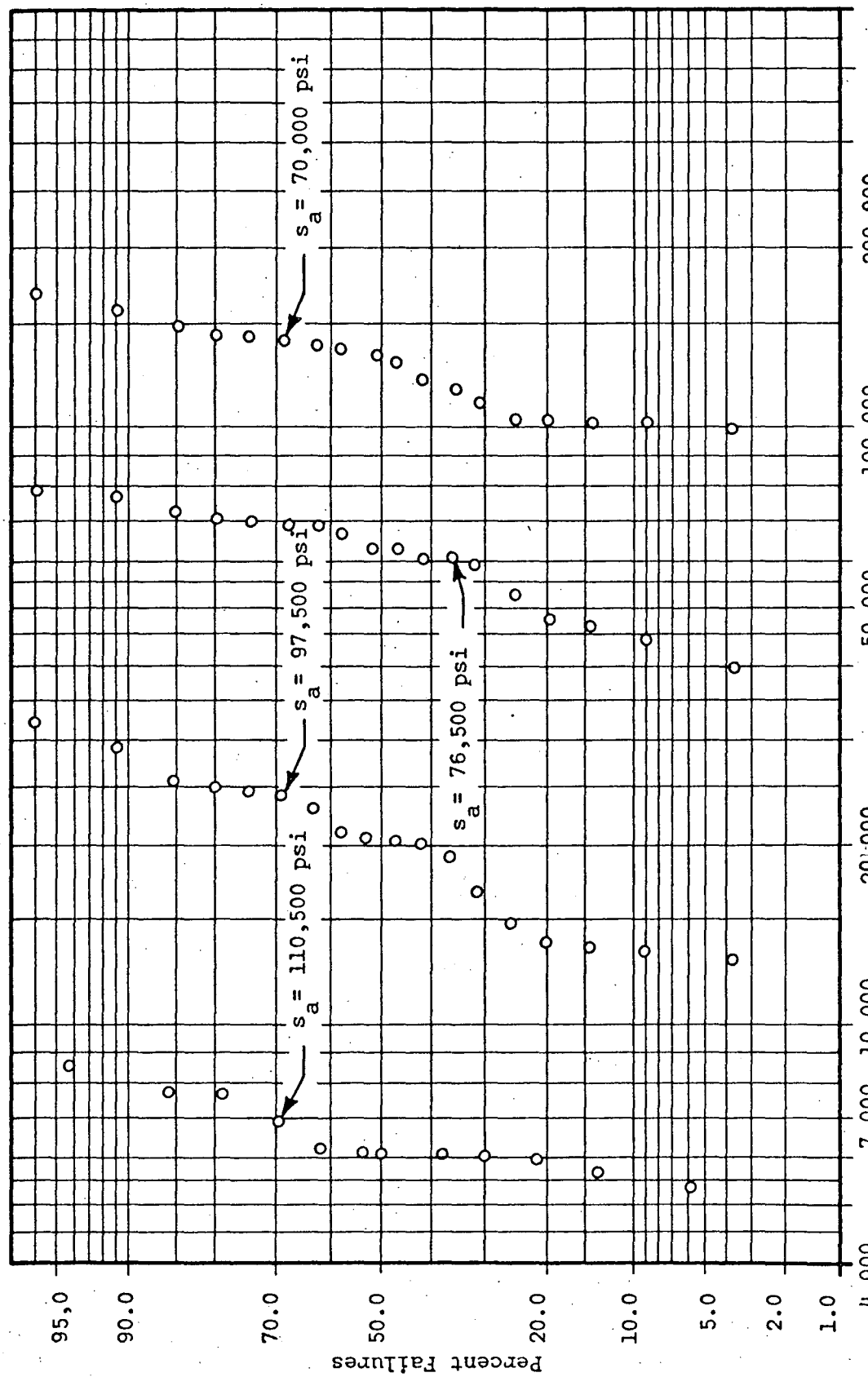

FIGURE 11. CYCLES-TO-FAILURE DATA FOR BENDING STRESSES OF 110,500 PSI, 97,500 PSI, 76,500 PSI AND 70,000 PSI AT STRESS RATIO 0.70 PLOTTED ON LOGNORMAL PROBABILITY PAPER.

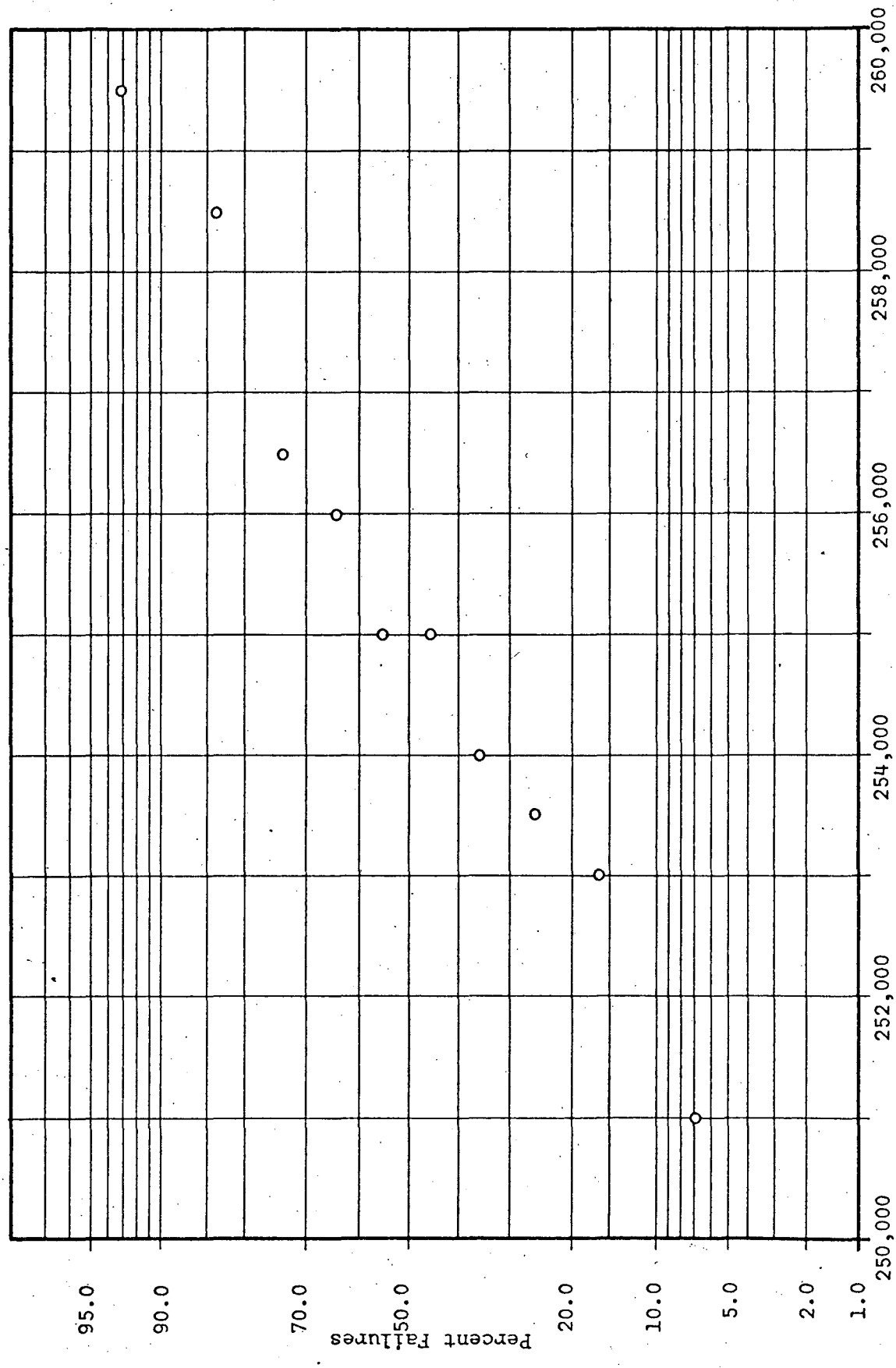

FIGURE 12. STATIC TENSILE ULTIMATE STRENGTH DATA FOR NOTCHED SPECIMENS PLOTTED ON NORMAL PROBABILITY PAPER.

CYCLES-TO-FAILURE FATIGUE DATA FOR SAE 4340 STEEL,
MIL-S-5000B, CONDITION C4 ROCKWELL C 35/40
FOR STRESS RATIOS OF ∞ and 0.70

Stress Ratio	r = ∞					r = 0.70			
Mean						0.722	0.703	0.682	0.709
Variability*						0.022	0.056	0.042	0.031
Coefficient of variation** (%)						3.1	8.0	6.2	4.3
Stress Level	****								
Mean (psi)	154,000	121,500	104,500	87,000	78,000	110,500	97,500	76,500	70,000
Variability (psi)	1,500	1,000	2,800	1,000	1,900	1,400	5,500	2,800	1,800
Coefficient of variation (%)	1.0	0.8	2.7	1.1	2.4	1.2	5.6	3.7	2.5
Cycles-to-Failure	***								
	1,650	7,100	16,250	60,000	93,300	5,400	12,950	39,550	99,400
	1,950	7,600	16,500	64,850	103,400	5,650	13,050	43,900	100,900
	2,450	7,700	17,000	65,000	124,150	5,900	13,350	46,450	101,200
	2,750	8,000	18,100	67,750	125,950	6,050	13,850	47,550	103,850
	2,900	9,000	19,350	71,150	127,800	6,100	14,900	52,700	104,350
	2,950	8,400	20,600	71,550	145,800	6,100	16,700	58,350	110,850
	2,950	8,850	21,100	71,950	155,200	6,150	19,100	60,000	117,950
	3,050	8,950	21,200	73,100	172,300	2,200	20,200	61,800	120,550
	3,050	9,100	21,200	74,700	172,550	6,900	20,200	62,250	129,250
	3,200	9,250	22,550	74,700	172,650	7,800	20,450	65,850	131,950
	3,200	9,300	22,900	75,650	177,500	7,800	21,000	67,500	135,950
	3,250	9,350	23,650	78,850	178,200	8,600	23,100	67,600	137,300
		9,750	24,300	82,250	182,850		24,350	69,150	140,350
		9,800	25,200	83,800	183,300		24,650	70,200	142,400
		10,000	27,000	86,350	195,800		25,000	72,000	143,200
		10,350	27,240	96,000	196,900		25,150	75,800	149,950
		10,350	27,450	98,450	203,000		28,250	77,850	159,300
		10,550	27,550	107,400	205,050		32,100		167,750

*The variability is the standard deviation of the distribution about the mean.
**The coefficient of variation is the ratio of the variability to the mean expressed as a percentage.
***All cycles-to-failure rounded to the nearest 50 cycles.
****All stresses rounded to the nearest 500 psi.

TABLE 2

STATIC ULTIMATE AND BREAKING STRENGTH DATA AND RESULTS FOR NOTCHED SPECIMENS*

(Stress ratio = 0)

Test No.	Ultimate Load 1000 lbs.	Breaking Load 1000 lbs.	Ultimate Strength psi. **	Breaking Strength psi. **
1	49.3	47.0	253,500	305,000
2	49.6	47.0	255,000	305,000
3	49.4	46.3	254,000	299,500
4	50.3	47.4	259,000	299,500
5	48.8	46.0	251,000	306,500
6	49.2	46.0	253,000	302,500
7	49.6	46.8	255,000	304,500
8	49.8	47.1	256,000	305,500
9	50.5	47.7	260,000	309,500
10	49.9	47.5	256,500	302,000

Normal Distribution Parameters of Ultimate Strength of Notched Specimens:

Mean = $\bar{S}_{Un}$ = 255,500 psi

Standard Deviation = $\sigma_{S_{Un}}$ = 2,500 psi

Normal Distribution Parameters of Breaking Strength of Notched Specimens:

Mean = $\bar{S}_{Bn}$ = 304,000 psi

Standard Deviation = $\sigma_{S_{Bn}}$ = 3,000 psi

*Specimen diameter at the base of the notch is 0.4975 in. which gives an area of 0.1944 sq. in.

**All strengths rounded to nearest 500 psi.

TABLE 3

STATIC YIELD, ULTIMATE AND BREAKING STRENGTH DATA AND RESULTS FOR UNNOTCHED SPECIMENS
(Stress ratio = 0)

Test No.	Yield Load 1000 lb	Ultimate Load 1000 lb	Breaking Load 1000 lb	Diameter Average, In.	Area Average $In.^2$	Yield Strength psi*	Ultimate Strength psi*	Breaking Strength psi*
1	31.5	32.5	24.3	0.4753	0.1774	177,500	183,000	264,000
2	30.6	31.5	23.5	0.4764	0.1784	171,500	176,500	254,000
3	30.6	31.6	23.3	0.4754	0.1775	172,500	178,000	249,000
4	20.8	31.0	22.8	0.4755	0.1776	168,000	174,500	251,500
5	29.9	31.1	22.9	0.4758	0.1778	168,000	175,000	254,500
6	30.1	31.3	23.2	0.4722	0.1752	172,000	178,500	256,500
7	30.4	32.5	25.0	0.4787	0.1800	169,000	181,000	256,000
8	30.2	31.4	24.2	0.4757	0.1777	170,000	178,000	253,000
9	30.6	31.6	23.6	0.4763	0.1782	172,000	177,500	259,000
10	30.3	31.2	24.2	0.4755	0.1766	171,000	176,500	250,500

Normal Distribution Parameters of Yield Strength of Unnotched Specimens:

Mean = $\bar{S}_{Yu}$ = 171,000 psi Standard Deviation = $\sigma_{S_{Yu}}$ = 3,000 psi

Normal Distribution Parameters of Ultimate Strength of Unnotched Specimens:

Mean = $\bar{S}_{Uu}$ = 178,000 psi Standard Deviation = $\sigma_{S_{Uu}}$ = 2,500 psi

Normal Distribution Parameters of Breaking Strength of Unnotched Specimens:

Mean = $\bar{S}_{Bu}$ = 255,000 psi Standard Deviation = $\sigma_{S_{Bu}}$ = 4,500 psi

*All strengths rounded to the nearest 500 psi.

TABLE 4

STRAIGHT LINE FIT AND CORRELATION COEFFICIENTS FOR NORMAL AND LOGNORMAL FITS TO CYCLES-TO-FAILURE DATA FOR STRESS RATIOS OF ∞ AND 0.70, AND STRESS-TO-FAILURE DATA FOR STRESS RATIO OF 0.

Stress Ratio	Stress Level (psi)	Best Fit for Normal	Best Fit for Lognormal	Correlation Coefficient	
				Normal	Lognormal
∞	154,000	Y=490x+2,780	Y=600x+2,730	0.9022	0.8724
∞	121,500	Y=1,070x+9,030	Y=1,150x+8,970	0.9869	0.9821
∞	104,500	Y=3,950x+ 22,170	Y=4,370x+21,850	0.9797	0.9772
∞	87,000	Y=12,750x+77,980	Y=13,300x+77,085	0.9612	0.9786
∞	78,000	Y=34,900x+161,980	Y=41,690x+158,100	0.9631	0.9426
0.70	110,500	Y=1,000x+6,550	Y=1,040x+6,490	0.9291	0.9435
0.70	97,500	Y=5,780x+20,470	Y=6,620x+19,730	0.9779	0.9752
0.70	76,500	Y=11,550x+61,030	Y=13,230x+59,990	0.9818	0.9665
0.70	70,000	Y=21,930x+127,580	Y=23,710x+125,910	0.9777	0.9763
0	-	Y=255,360x+2,830	Y=255,350x+2,843	0.9891	0.9894

APPENDIX A-1

CONVERSION OF TIMES-TO-FAILURE DATA TO CYCLES-TO-FAILURE FOR 154,000 PSI ALTERNATING STRESS AND STRESS RATIO ∞

Item No.	Spec. No.	Machine No.	Time to Failure hr:min:sec	Cycles to Failure	Log_e Cycles	Median Ranks *
1	341	1	0:00:56	1,667	7.4188	5.613
2	365	1	0:01:05	1,935	7.5678	13.598
3	342	1	0:01:23	2,471	7.8124	21.669
4	193	2	0:01:33	2,765	7.9248	29.758
5	196	2	0:01:37	2,884	7.9669	27.853
6	204	2	0:01:40	2,973	7.9973	45.951
7	166	2	0:01:40	2,973	7.9973	54.049
8	133	2	0:01:42	3,033	8.0173	62.147
9	225	2	0:01:43	3,063	8.0271	70.242
10	220	2	0:01:47	3,182	8.0653	78.331
11	191	2	0:01:47	3,182	8.0653	86.402
12	163	2	0:01:50	3,271	8.0929	94.387

*(17, Table I)

APPENDIX A-2

CONVERSION OF TIMES TO FAILURE DATA TO CYCLES-TO-FAILURE FOR 121,500 PSI ALTERNATING STRESS AND STRESS RATIO ∞

Spec. No.	Machine No.	Time to Failure	Cycles to Failure	Log_e Cycles	Median Ranks
96	1	Cycles measured directly with positively driven revolution counter.	7,112	8.8695	3.778
86	1		7,622	8.9388	9.151
69	1		7,717	8.9512	14.581
89	1		8,015	8.9891	20.024
22	1		8,088	8.9981	25.471
20	1		8,376	9.0331	30.921
76	1		8,860	9.0893	36.371
111	1		8,925	9.0966	41.828
101	1		9,092	9.1151	47.274
73	1		9,261	9.1336	52.726
64	1		9,302	9.1380	58.177
80	1		9,362	9.1444	63.629
52	1		9,747	9.1874	69.079
59	1		9,818	9.1920	74.529
109	1		9,990	9.2093	79.976
82	1		10,347	9.2444	85.419
42	1		10,353	9.2450	90.849
63	1		10,540	9.2630	96.222

APPENDIX A-3

CONVERSION OF TIME-TO-FAILURE DATA TO CYCLES-TO-FAILURE FOR 104,500 PSI ALTERNATING STRESS AND STRESS RATIO ∞

Cycles measured directly with positively driven revolution counter.

Spec. No.	Machine No.	Time to Failure	Cycles to Failure	Log_e Cycles	Median Ranks
39	1		16,258	9.6963	3.778
55	1		16,500	9.7111	9.151
99	2		16,920	9.7362	14.581
33	1		18,136	9.8056	20.024
71	1		19,352	9.8075	25.471
65	2		20,576	9.9319	30.921
46	2		21,080	9.9561	36.371
85	2		21,192	9.9614	41.823
113	1		21,204	9.9619	47.274
26	1		22,544	10.0232	52.726
49	2		22,886	10.0383	58.177
110	1		23,640	10.0707	63.629
82	2		24,304	10.0984	69.079
13	2		25,196	10.1344	74.529
58	1		27,024	10.2045	79.976
88	1		27,250	10.2128	85.419
62	2		27,464	10.2206	90.849
104	2		27,558	10.2241	96.222

APPENDIX A-4

CONVERSION OF TIMES-TO-FAILURE DATA TO CYCLES-TO-FAILURE FOR 86,000 PSI ALTERNATING STRESS AND STRESS RATIO ∞

Spec. No.	Machine No.	Time to Failure	Cycles to Failure	Log_e Cycles	Median Ranks
45	1	Cycles measured directly with positively driven revolution counter.	60,002	11.0021	3.778
94	1		64,857	11.0799	9.151
102	1		64,997	11.0821	14.581
118	1		67,757	11.1237	20.024
114	1		71,166	11.1728	25.471
29	1		71,556	11.1782	30.921
35	1		71,968	11.1840	36.371
18	1		73,089	11.1994	41.823
25	1		74,690	11.2211	47.274
30	1		74,698	11.2212	52.726
31	1		75,662	11.2340	58.177
34	1		78,852	11.2753	63.629
70	1		82,248	11.3175	69.079
75	1		83,812	11.3363	74.529
66	1		86,349	11.3662	79.976
48	1		96,004	11.4722	85.419
19	1		98,468	11.4975	90.849
81	1		107,415	11.5845	96.222

APPENDIX A-5

CONVERSION OF TIMES-TO-FAILURE DATA TO CYCLES-TO-FAILURE FOR 78,000 PSI ALTERNATING STRESS AND STRESS RATIO ∞

Spec. No.	Machine No.	Time to Failure	Cycles to Failure	Log_e Cycles	Median Ranks
215	2	0:52:18	93,303	11.4436	3.718
167	2	0:57:58	103,413	11.5465	9.151
121	2	1:09:35	124,137	11.7292	14.581
135	2	1:10:36	125,950	11.7436	20.024
145	2	1:11:38	127,794	11.7582	25.471
198	2	1:21:43	145,783	11.8899	30.921
128	2	1:26:59	155,178	11.9523	36.371
156	2	1:36:34	172,275	12.0569	41.823
171	2	1:36:44	172,572	12.0586	47.274
123	2	1:36:47	172,662	12.0591	52.726
159	2	1:39:30	177,508	12.0868	58.177
134	2	1:39:53	178,192	12.0906	63.629
183	2	1:42:30	182,860	12.1165	69.079
186	2	1:42:45	183,306	12.1189	74.529
214	2	1:49:46	195,824	12.1850	79.976
125	2	1:50:22	196,894	12.1904	85.419
148	2	1:53:48	203,019	12.2211	90.849
219	2	1:54:56	205,041	12.2310	96.222

APPENDIX A-6

CONVERSION OF TIMES-TO-FAILURE DATA TO CYCLES-TO-FAILURE FOR 110,500 PSI ALTERNATING STRESS AND STRESS RATIO 0.70

Spec. No.	Machine No.	Time to Failure	Cycles to Failure	Log_e Cycles	Median Ranks
397	1	0:03:01	5,388	8.5919	5.613
395	1	0:03:09	5,626	8.6351	13.598
432	1	0:03:18	5,894	8.6817	21.669
387	1	0:03:23	6,043	8.7067	29.758
335	1	0:03:24	6,072	8.7114	37.853
358	1	0:03:25	6,102	8.7164	45.951
356	1	0:03:27	6,162	8.7262	54.049
392	1	0:03:29	6,221	8.7357	62.147
354	1	0:03:52	6,906	8.8401	70.242
406	1	0:04:22	7,799	8.9617	78.331
390	1	0:04:23	7,899	8.9656	86.402
345	1	0:04:49	8,603	9.0599	94.387

APPENDIX A-7

CONVERSION OF TIMES-TO-FAILURE DATA TO CYCLES-TO-FAILURE FOR 97,500 PSI ALTERNATING STRESS AND STRESS RATIO 0.70

Spec. No.	Machine No.	Time to Failure	Cycles to Failure	Log_e Cycles	Median Ranks
254	3	0:07:17	12,964	9.4699	3.778
423	1	0:07:18	13,038	9.4756	9.151
408	1	0:07:29	13,365	9.5004	14.581
379	1	0:07:45	13,842	9.5355	20.024
367	1	0:08:20	14,883	9.6080	25.471
370	1	0:09:21	16,699	9.7231	30.921
314	3	0:10:44	19,105	9.8577	36.371
237	2	0:11:19	20,189	9.9129	41.823
307	3	0:11:21	20,203	9.9136	47.274
292	2	0:11:28	20,457	9.9261	52.726
261	2	0:11:48	21,004	9.9526	58.177
256	3	0:12:59	23,110	10.0480	63.629
274	3	0:13:41	24,356	10.1005	69.079
262	3	0:13:51	24,653	10.1127	74.529
312	3	0:14:03	25,009	10.1270	79.976
258	3	0:14:08	25,157	10.1329	85.419
227	3	0:15:52	28,243	10.2486	90.849
295	3	0:18:03	32,129	10.3775	96.222

APPENDIX A-8

CONVERSION OF TIMES-TO-FAILURE DATA TO CYCLES-TO-FAILURE FOR 76,500 PSI ALTERNATING STRESS AND STRESS RATIO 0.70

Spec. No.	Machine No.	Time to Failure	Cycles to Failure	Log_e Cycles	Median Ranks
382	1	0:22:09	39,560	10.5856	3.778
441	1	0:24:36	43,936	10.6905	9.151
416	1	0:26:01	46,466	10.7465	14.581
405	1	0:26:38	47,567	10.7699	20.024
471	1	0:29:30	52,687	10.8721	25.471
363	1	0:32:41	58,372	10.9746	30.921
141	1	0:33:35	59,980	11.0018	36.371
427	1	0:33:35	59,980	11.0018	41.823
285	3	0:34:43	61,796	11.0316	47.274
404	1	0:34:51	62,242	11.0388	52.726
200	1	0:36:52	65,844	11.0981	58.177
154	1	0:37:51	67,491	11.1214	63.629
277	3	0:37:55	67,600	11.1298	69.079
185	1	0:38:43	69,184	11.1440	74.529
218	1	0:39:18	60,190	11.1590	79.976
176	1	0:40:19	72,006	11.1845	85.419
326	3	0:42:35	75,798	11.2358	90.849
172	1	0:43:35	77,840	11.2624	96.222

APPENDIX A-9

CONVERSION OF TIMES-TO-FAILURE DATA TO CYCLES-TO-FAILURE FOR 70,000 PSI ALTERNATING STRESS AND STRESS RATIO 0.70

Spec. No.	Machine No.	Time to Failure	Cycles to Failure	Log_e Cycles	Median Ranks
272	3	0:55:50	99,383	11.5067	3.778
385	1	0:56:29	100,879	11.5217	9.151
321	3	0:56:51	101,193	11.5248	14.581
360	1	0:58:09	103,856	11.5508	20.024
327	3	0:58:38	104,367	11.5557	25.471
442	1	1:02:04	110,851	11.6160	30.921
268	3	1:06:16	117,955	11.6781	36.371
229	3	1:07:44	120,565	11.7000	41.823
304	3	1:12:36	129,228	11.7693	47.274
230	3	1:14:08	131,957	11.7902	52.726
231	3	1:16:23	135,962	11.8201	58.177
228	3	1:17:09	137,327	11.8301	63.629
337	1	1:18:35	140,350	11.8519	69.079
413	1	1:19:44	142,404	11.8664	74.529
247	3	1:20:27	143,201	11.8720	79.976
287	2	1:24:03	149,945	11.9180	85.419
255	3	1:29:29	159,280	11.9784	90.849
232	3	1:34:14	167,735	12,0301	96.222